

IDENTIFICATION QUANTIFICATION AND MAPPING OF BLACK CARBON USING GITs



FINAL YEAR PROJECT UG-2020

By

Leader-333132-Dua Saleem

Member 1-332158-M. Saleem Siddiqui

Member 2-341592-Monaima Farooq

Member 3-332630-USama Zahid

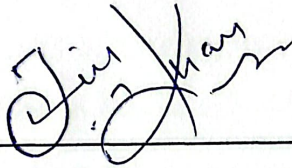
Supervisor: Mr Junaid Aziz Khan

**Institute of Geographic Information Systems
School of Civil and Environmental Engineering
National University of Science and Technology
Islamabad, Pakistan**

Certificate

Certified that the contents and form of thesis entitled “**IDENTIFICATION QUANTIFICATION AND MAPPING OF BLACK CARBON USING GITs**” submitted by Ms. Dua Saleem, Mr. Saleem Siddiqui, Mr. Usama Zahid, Ms. Monaima Farooq have been found satisfactory for the requirement of the degree.

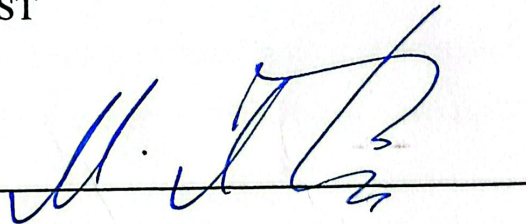
Supervisor: _____



(Junaid Aziz Khan)

Lecturer- IGIS, SCEE, NUST

Head of Department: _____



(Muhammad Azmat)

Lecturer- IGIS, SCEE, NUST

STATEMENT BY THE AUTHORS

It is declared that this thesis and the work presented in it are our own and have been generated by us as the result of our own research.

“IDENTIFICATION AND QUANTIFICATION OF BLACK CARBON USING GITs”

We confirm that:

1. This thesis is composed of our original work and no material previously published or written by another person except where due reference has been made in the text.
2. Wherever any part of this thesis has previously been mentioned for a degree or any other qualification at this or any other institution, it has been clearly mentioned.
3. I have acknowledged all main sources of help.
4. This work has been presented as combined effort of the whole group, where everyone contributed his best.
5. None of the work has been published before submission.
6. This work is not plagiarized under HEC plagiarism policy.

Signatures of Group Members:

Dua Saleem, IGIS-NUST

Saleem Siddiqui, IGIS-NUST

Monaima Farooq, IGIS-NUST

Usama Zahid, IGIS-NUST

ACKNOWLEDGEMENT

We are extremely pleased that we had your support during our thesis, and we are forever grateful for it. A special shoutout to Mr. Junaid Aziz Khan whose indispensable guidance we couldn't have done without in this research trip – he was our light in pitch-dark areas.

If it weren't for your continuous support from our families, our friends, our loved ones and National University of Science and Technology, our whole world would have been different. Your love, understanding as well as monetary support turned out as an enabling factor that allowed us to score good grades.

In addition, for all the compassionate people who donated with their time and expertise, Thank you. We would like to express our gratitude for the assistance you rendered. Our research benefited greatly from your knowledge and experience when working together.

It was a personal accomplishment at the same time being the dedication to the teamwork and support of those around me. We are most sincerely grateful that you are a part of this adventure with us!

SUSTAINABLE DEVELOPMENT GOALS

Our project meets 3 of 17 sustainable development goals set forward by the United Nations in 2015.



ABSTRACT

The research focuses on black carbon (BC), one of the major environmental and health impairments that are emitted as a result of incomplete combustion. Additionally, the small size of (BC) black carbon and its light-absorbing ability is one of the main components leading to global warming, and adverse health effects. Though its influence is huge, the current monitoring methods lack the cost effectiveness and efficiency to a greater extent. To overcome this gap, a cheap and efficient device is developed for finding the BC measurements by using Geospatial Integrated Technologies (GIT's). The invention of the black carbon detecting device, is used for detecting and finding black carbon (BC) concentration in the air, and is based on a unique method and technology. IR and RGB LEDs, and LDR sensors are connected in the both ends of the parallel section of a U-shaped tube to analyse BC particles. Subsequently, they are connected through Arduino Nano, which communicates to DHT sensors delivering data of temperature and humidity, and GPS unit which displays the location data and PMS5003 sensor for finding particulate matter concentrations. Results are shown on LCD screen for user convenience. The data from each sensor is stored in excel and displayed in GUI and is visualized through heat maps made in ArcGIS Pro and statistical dashboard made in tableau that displays the black carbon per minute concentrations and each LED data recorded by LDR. The LDR data obtained from both chambers, one before filtration and other after filtration of black carbon is monitored to quantify black carbon particles in the air. By comparing the results of the black carbon detecting device with aethalometer and measuring the R Square and Mean Absolute Percent Error (MAPE) through three different machine learning algorithms shows an accuracy of 94%.

LIST OF ACRONYMS

GITs: Geospatial Information Technologies

ABCD: Aerosol Black Carbon Detector

BC: Black Carbon

SLCP: Short Lived Climate Pollutant

GHG's: Green House Gasses

GWP: Global Warming Potential

HSV: Hue, Saturation, Value

LED: Light Emitting Diode

LDR: Light Dependent Resistor

NIOSH: National Institute for Occupational Health and Safety

US EPA: United States Environmental Protection Agency

PASS: Photoacoustic Smoke Sensor

MAPE: Mean Absolute Percent Error

rBC: Refractory Black Carbon

EBC: Equivalent Black Carbon

DOM-BC: Digital Optical Method for Black Carbon

LIST OF TABLES AND FIGURES

Table 3.1.1- Materials and Equipment.....	21
Figure 3.1: Design Workflow	22
Figure 3.2: Methodological framework	23
Figure 3.3: Shows device workflow	25
Figure 3.4: Code Implementation of GP	26
Figure 3.5: Code Implementation of DHT.....	26
Figure 3.6: Code Implementation of LCD	27
Figure 3.7: Code Implementation of PMS 5003	28
Figure 3.8: Code Implementation of PMS 5003	28
Figure 3.9: Code Implementation of LDR.....	29
Figure 3.10: Code Implementation of LED	30
Figure 3.11: Shows first design	30
Figure 3.12: Shows second design.....	32
Figure 3.13: Shows final design	33
Figure 3.14: Shows circuit design	34
Figure 4.1: Shows complete design with aethalometer	35
Figure 4.2: Shows complete design with aethalometer	36
Figure 4.3: Shows device internal structure	36
Figure 4.4: Data in Excel.....	36
Figure 4.5: Dashboard.....	37
Figure 4.6: Shows code implementation of GUI interface in python	39
Figure 4.7: Shows code implementation of GUI interface in python	40
Figure 4.8: Shows GUI interface in python	40
Figure 4.9: Shows study area	41
Figure 4.10: Shows heat map of study area	42
Figure 4.11: Code Implementation of training data and accuracy assessment.....	43
Figure 4.12: Code Implementation of training data and accuracy assessment	43

Figure 4.13: Result for gradient boosting algorithm	43
Figure 4.14: Shows best fit line graph	44
Figure 4.15: Code Implementation of training data and accuracy assessment.....	45
Figure 4.16: Code Implementation of training data and accuracy assessment.....	46
Figure 4.17: Results for Random Forest Algorithm	46
Figure 4.18: Shows best fit line	47
Figure 4.19: Code implementation for training data and test data.....	48
Figure 4.20: Code implementation for training data and test data.....	49
Figure 4.21: Result for XG Boost Algorithm.....	49
Figure 4.22: Shows best fit line	50
Figure 4.23: Shows validation of data by observing and combining data from aethalometer and Device	51

TABLE OF CONTENTS

STATEMENT BY THE AUTHOR.....	3
ACKNOWLEDGMENTS.....	4
SUSTAINABLE DEVELOPMENT GOALS.....	5
ABSTRACT.....	6
LIST OF ACRONYMS.....	7
TABLES.....	8
TABLE OF CONTENT.....	9
LIST OF FIGURES.....	11
CHAPTER 1- INTRODUCTION.....	12
1.1 General overview.....	12
1.2 Black Carbon Formation.....	12
1.3 Physical Properties.....	12
1.4 Environmental Impacts.....	12
1.5 Health Effects.....	12
1.6 Contribution to Climate Change.....	13
1.7 Problem Statement.....	13
1.8 Objectives.....	13
CHAPTER 2- LITERATURE REVIEW.....	14
CHAPTER 3- MATERIALS AND METHODS.....	21
3.1 Materials.....	21
3.2 Methodology Flowchart.....	22
3.3 Methodology for ABCD.....	23
3.4 Equipment.....	25
3.5 Testing and Validation.....	30
CHAPTER 4- RESULTS AND DISSCUSSION.....	35
4.1 Field Test.....	35
4.2 Device Mechanism Setup.....	35
4.3 Data Storage.....	36
4.3.1 Excel.....	36
4.4 Visualization.....	37
4.4.1 Dashboard.....	37
4.4.2 Python GUI.....	37
4.4.3 Study Area.....	41

4.4.4 Heatmap	41
4.5 Accuracy Assessment and Validation	42
CHAPTER 5- CONCLUSIONS	52
CHAPTER 6- RECCOMENDATION	53
CHAPTER 7-BENEFICIARIES	54
REFRENCES	55

CHAPTER 1

INTRODUCTION

1.1 General overview:

Black carbon defines abrasion particles of carbon, which is emitted due to imperfect burning of oil, biomass, and biofuel. These particles are often in the form of soot with diameters below 2.5 micrometres (PM_{2.5}), the case is recently more complicated and of great concern.

1.2- BC Formation:

They are produced in the process of incomplete burning of fossil fuels, biofuels, and biomass. Hence, they also play a major role in air pollution. These kinds of emissions occur because of automobiles and industrial processes, wildfires, and burning of fuelwood as well as residential cooking and space heating. Such aerosols are usually in a soot form and are extremely small. In lesser than 2,5 micrometres (PM_{2.5}) they are even smaller.

1.3-Physical Properties:

The black carbon particles being very dark and opaque absorb the sun's radiation over ultraviolet to infrared ranges of the light spectrum. They may rest there for long stretches, which contributes to the fact they may be transported across large distances.

1.4-Environmental Impacts:

Coal soot has got evidence that it plays large environmental role. Landing on snow and ice, it lowers the surfaces albedo, which name ice and snow melting at higher speed and contributes to global warming. In the atmosphere black carbon can absorb sunlight directly, which challenges local climate by enhancing local temperature turbulence.

1.5-Health Effects:

Inhalation of black carbon particles is very harmful and the respiratory and cardiovascular systems, can be adversely affected. Among the most detrimental effects is the fact that these particles are so tiny that they can go in deeper into the lungs and get into the bloodstream stimulating inflammation and making the health problems worse.

1.6-Contribution to climate change:

Compared to longer-lived greenhouse gases like carbon dioxide (CO₂), black carbon is classified as a short-lived climate pollutant (SLCP). Even while black carbon has a limited lifespan, it nevertheless has a very strong warming impact.

According to the estimates, it is the second-largest greenhouse gas after carbon dioxide (CO₂).
Undefined The direct effect: Through this process the sunlight coming from the sun is absorbed by the BC that diffuses in the atmosphere as a result. As the concentration of BC goes up there is a reduction in the planetary albedo and the amount of solar energy that reaches the ground is reduced by around 25 Wm⁻² or about 5% (Krishnan and Ramanathan, 2002). In other words, BC is a cause of the so called “global dimming” (Stanhill and Cohen, 2001). The changes in surface fluxes of heat and moisture are a result of that (Ramanathan et al., 2001). The surface radiation change can reach three times the level at top of the atmosphere. The indirect effect: BC nucleated or scavenged within other aerosols can affect microphysics of clouds and changes a drop size. The semi-direct effect: Many studies conducted over the Indian Ocean, North America and model shows that the atmospheric absorption rates increase by as much as 1 to 3 K per day (Ackerman et al., 2000, Koren et al., 2004, Johnson et al., 2004). This led to the changes in humidity profiles involved in cloud persistency and formation. The indirect surface Albedo: Warming of snow and glaciers can be caused by BC which will melt the snow, resulting in flooding. Black carbon concentration measurement in the air is essential for understanding its trace sources, distribution and influences on both climate and air quality.

1.7-Problem statement:

Despite being able to get a rough estimate about how much BC there is in the atmosphere, there is no working and exact way, at least in the short term, of identifying and monitoring black carbon.

1.8-Objectives:

The aim of this study is to fabricate and implement an optimal device for the identification and measurement of black carbon (BC) in the atmosphere, with initial deployment at the National University of Sciences and Technology (NUST) campus in Islamabad, Pakistan using rapid sampling techniques and GIT applications that are cost effective and efficient.

CHAPTER 2

LITERATURE REVIEW

Olson et al., (2016) states a fast and budget-maximizing colour identification application will be used for colour evaluation of collected media in water filters to calculate organic carbon (EC/OC) content, disturbance loads, etc. This method to predict OC composition is the first of its kind that utilizes SPH to update concentrations after different time steps. Colorimetry and digital photography are exploited to derive the moisture content expressed in Estimated NIOSH and Improve TOR EC/OC. When compared with an HSZ VOC monitoring system over an assay time of 315 samples, our HSV VOC measurement model reveals that it is an effective way to monitor HSV with $R^2 = 0.917$ estimated ratio and higher CV (rms error) for measured values (16.1%). Specifically, the Ciudad de los Veteranos, built with the similar filter design, has R^2 equals 0.671 and 24.8% of the deviation is modelled using the measurements. A similar approach was taken on the dataset of NIOHS EC/F concentrations for dust samples from the rural areas of China, Baghdad and in San Joaquin Valley, California, where the CV (RMSE) values were 30.8% and 49.3% respectively for the EC and the OC. Moreover, the author uses the same strategy for the samples whose colour was measured with DPI method, and the results of the EC implied a good agreement with standard p-I (RMSE) of 22.6%. The LP-DPI technique unfortunately did not fulfill the promise of accurately measuring the OC level, which was verified with a CV (RMSE) of 77.5%. The low cost is thus a big benefit of that tool, since it allows exposure level estimates to be made in developed places and the scale of the projects be monitored.

Krämer et al., (2002) states that a Mobile Photoacoustic Smoke Sensor (PASS), which is an adaptation of the previous device, has been developed and used in this study to ensure feed of air particulate online in real-time. 19-inch sensor BC device for the house the standard calibration was done with lead to $0.27 \mu\text{V}$ per $\mu\text{g m}^{-3}$ which gave detection limit of about 200 ng m^{-3} by measure time. Cross-susceptibility with other air constituents was then examined, and it was detected that water, NO_2 , and light-emitting particles were the main contributors. Time period is inferior to few minutes. An auto measurement cycle (ideal for emissions detection) is a function that can take the time from 5 minutes to program. Knowing the BC mass distribution both inside and outside of the atmosphere is critical to studying the health effects of planetary forcing.

The requirements for suitable equipment for carbon black monitoring are as follows: The requirements for suitable equipment for carbon black monitoring are as follows:

1. outstanding sensitivity or detecting down to $1 \mu\text{g m}^{-3}$ level.
2. high selectivity.
3. fast response time
4. mobility.

There is a large range of monitoring methods which do the task, but at the same time, there is no method which can do its job perfectly, as all the above-mentioned conditions cannot be simultaneously met. Unfortunately, determination of BC concentration with instruments operating by the optical method (e.g. a photometer 2) is limited by its sensitivity to light-scattered particles and the filter-matrix narrowing of particle concentration. Thus, an in-depth calibration would be more accurate. In contrast, filtration that has been on for the long term should carry out with atmospheric soot using a thermal analyser approach like coulometric method 2. The results may not be selective; include non-volatile and non-extractable organic carbon such as pollen or humic acids. Determined carbon content). The atmospheric BC determination using photoacoustic (PA) spectroscopy by Petzold and Nieserⁿ has shown it to be a very effective method, which offers a detection limit of around $1 \mu\text{g m}^{-3}$, an integration problem in the order of minutes, in addition to providing a solution to optical efficiencies problems. The spores and particles of the design process are small, so the particles are scattered. The detection of BC by a photoacoustic imaging system is based on multiple repetitions of visible light absorption and heat transfer from energy absorption to the gas through the way of non-electrical relaxation of the excited substance lying in only one cycle. On the contrary, pressure shift of gas molecules in the container can be followed by a microphone turning them into a signal equal to the grateful group concentration. The high sensitivity of BC will be attained attributing to the following reasons. First large among BC particles absorption cross section can be achieved. Secondly, we will use a powerful diode laser. Thirdly, the use of resonance amplification of acoustic waves in the photoacoustic cell will be essential. In the end, the choice of carefully selected microphones is also relevant electronic. The second work is a progress of the Photoacoustic Soot Sensor (PASS) 3 which have been aimed to make it kind enough for emission measurement.

Caubel et al., (2018) states that ambient air quality monitoring has historically involved the use of only a few dedicated remote reference stations with high-cost, precision etc referenced

instrumentation. These reference stations, however, may not be sufficient to characterize spatial distribution of pollutants, although such data are critical in setting the trend of air pollution; especially in urban areas where changes in pollution concentrations could be rapid within small distances. This is a limitation especially for BC together with other types of PMs that have serious health and climate implications. Despite the recent improvement in BC monitor technologies, they are generally expensive, costing between \$10,000 to \$20,000; this has limited their use hence the gaps in information about BC distribution across diverse areas. Low-cost air pollution sensors have recently emerged as a tool of increasing importance in the air quality assessment field. Such sensors, which are usually costing between a few hundred dollars up to a few thousand dollars, have made it possible for designers to install vast networks of sensors that will allow for high resolution data collection. To this end, such networks are more frequently utilized for the assessment of different air pollutants like nitrogen dioxide (NO₂), ozone (O₃), and particulate matter (PM). These have helped in the development of more precise readings of air pollution giving information that could not be realized by conventional monitoring. BC is one of the major elements of PM that mainly originates from excessive use of fossil fuels and biomass burning. Due to its function being short-lived climate pollutant and the following health consequences it deserves a spot in air quality tracking. Nevertheless, the high cost and operation complexity of the currently available BC measurement tools are constraints that have hindered the implementation of these tools. Common BC analysers include aethalometer and particle soot absorption photometer and almost all of them rely on absorption of light to determine the concentration of BC. Nevertheless, these instruments are not intended for mass usage in the framework of intricate monitoring arrays because of the expense as well as the consideration that they demand constant servicing. Current advancements have targeted the improved BC sensors that are cheaper and easily deployable in large arrays for the purpose of attaining higher density coverage. These advancements are important in enhancing the ability to measure the BC at high-resolution at the traffic and industrial regions in the urban economies. The trend towards developing new devices that are capable of revealing aerosol black carbon density is in the right direction due to digital development. It also should be noted that ABCD is cost effective, easy to implement large-scale monitoring network in different environments. A key limitation of low-cost BC sensors like the ABCD is a number of interfering factors, including the dependence of the sensors' response on the environmental conditions, notably temperature and humidity. Prior research has pointed out that the deficiencies in treatment need to be accounted for by using appropriate pay methods that would increase the validity of BC measurements in

unconditioned contexts. The ABCD meets this challenge by adopting a new approach to data processing that eliminates complications occasioned by changes in temperatures when the sensor is used in outdoor environments. This is particularly beneficial in the measurement accuracy of BC gained in the densely monitored network since the environmental conditions in such networks can be highly dynamic. The performance of the ABCD has been further confirmed during the field trials, during which the system incorporating more than 100 units has been tested in parallel with a commercial BC instrument. The findings showed that ABCD has similar measurement accuracy and precision with those of expensive commercial instruments, with the fleet-average error within desired ranges for air quality assessment. These findings underscore the potential of the ABCD as a viable solution for expanding BC monitoring capabilities in dense sensor networks, providing high-resolution data that can inform public health interventions and environmental policy.

Petzold and Schönlinner, (2004) proposes a way of measuring light absorption by aerosols is suggested but based on the simultaneous collection of the transmitted (radio) and backscattered (radio) radiation by the particles in glass fibre filters. Here the influence of aerosol component on emission angle of back-radiation is examined by collecting data from three different angles. One of the principles behind the radiation absorption phenomenon in the particulate mass (radiative transfer theory) is the absorbance of a fraction of the light it encounters. A normalization was applied to the mass fraction of black carbon to analyse its connection to aerosols, specifically those with a light absorption coefficient between 1.2% and 100%. The scattering of aerosols was observed, and absorptiometry measurements were conducted, considering different angles and scattering conditions where scattering exceeded 300%, but was less than 50% in multiple cases. Researchers will work to develop advanced compensation for light scatter in filter-based measurements of light absorption. The detection rate is $3.5 \times 10 \times 4$ absorbance units, which is equivalent to 103. Absorbance uncertainty is $\pm 12\%$. By employing area specific data, the evaluation of this approach resulted in having an average sorption coefficient magnitude of -9.1 for atmospheric black carbon in urban air.

Highwood and Kinnersley, (2006) states that the same time space those different places became obvious and taken in that line climate change and climate change are the central points of political and social agenda in a local arrangement to the international one. Black carbon, chemically varied and attributed to a wide range of combustion processes, catches, and absorbs sunlight, thus enlarging the amount of suspended and unclean particles in the air and resulting in respiratory disorder and heart disease. The fact that black carbon may be found in large, but

variable amounts in many shapes and sizes renders the prediction of its climate effect a complex task for researchers. More data gathering brought to light new factors that affected matter, and there arose new uncertainties. While this is a subject covered widely across the available literature and experiments, we've also partnered with different institutions to boost our confidence concerning the extent of human health and environmental impacts that are associated with black carbon. Landmarks: it comprises correctly established information concerning the area, percentage, types, and quantitative data, etc.

According to Bahadur et al., (2012) aims at addressing the deficiency on black carbon as a major portion of TC, which comprise of elemental carbon (EC) and brown carbon (BrC), whereas the latter is seldom considered in climate models. To accomplish that, the study put forward an observationally based analysis technique to apportion AAOD and SSA between EC and BrC. Analysing the results, it can be noted that EC has very high levels of absorption whereas absorption levels of BrC varies at the global level. The point here is that the study has made practical applications for California where a TC made a magnificent showing concerning the total level of absorption and where BrC absorption depended on the season and geographic region, including forest fires. This study shows that current climate models underestimate the warming effects of carbonaceous aerosols by not including BrC, indicating that for accurate assessment of heat in the atmosphere, there is a need for models to integrate BrC absorption particularly in biomass- burning areas.

Caubel et al., (2019) states that in response to the difficulty in tracking loosely dispersed PM pollution, the research uses 24 low-cost BC sensors spread out across West Oakland, California. The 100 x 100 BC Network was set up with 100 BC sensors in 100 sites for 100 days in a 15 km² area influenced by freeways and industrial emissions. Many studies have been based on conventional regulatory monitors which are incapable of indicating the spatial distribution of pollutants in urban environments as achieved by low-cost sensor networks in this research. The findings presented focus on dispersion of BC concentrations which change with space and time depending on local traffic and industry emissions, and especially the variation is noticeable for short distances about 100m and short time intervals of about one hour. These findings also show the importance of dense sensor networks in the assessment of air pollution in urban areas since it is essential to develop effective measures of exposure to air pollutants in the built environment. The study also focuses on proper sensor hardware validation and data acquisition system certification before field implementation and finally recognizing the spirit of community involvement on the networks' effective deployment as well as management.

Sajjadi et al., (2017) assessed PM_{2.5} and PM₁₀ concentrations in Sabzevar, Iran, using measurements from 48 stations and applying spatial interpolation models including Radial Basis Functions (RBF), Inverse Distance Weighting (IDW), Ordinary Kriging (OK), and Universal Kriging (UK). The research found that pollutant levels often exceeded regulatory standards, with IDW emerging as the most accurate interpolation method based on lower MAPE values. The research highlights the urgent need for continuous monitoring and control of particulate matter emissions in urban areas to mitigate health risks.

Sharma et al., (2017) evaluated three methods for measuring black carbon (BC) at the Global Atmosphere Watch observatory in Alert, Canada: The obtained concentrations of equivalent black carbon (EBC) using an Aethalometer and elemental carbon (EC) via thermal desorption and of refractory black carbon (rBC) using a single particle soot photometer (SP2). The analysis of data shown that there was a difference in EBC and EC values which was significantly higher than rBC due to factors other than BC. The best assessment of BC mass was determined by the arithmetic mean of rBC and EC data, displayed seasonal changes during the time of this study. The study also revealed seasonality in mass absorption coefficients MACs for the observed aerosols across the different seasons with initial evidence of the relationship between MAC values and particle coating thickness; this further brings out the level of complexity and uncertainty when measuring black carbon in Arctic regions.

Cheng et al., (2011) attempt to find out the viability of employing digital imaging as a cost-effective solution in place of gravimetric approaches for analysing airborne elemental carbon (EC). Using an office scanner which resulted in an estimation of EC concentrations, RGB values of the blackness of aerosol-laden filters were gathered. The next data analysis revealed that the relation between the transformed RGB values and the EC loading is power-law with the mean absolute error of 10. Thus, the sensor's energy consumption is 3% less than in conventional thermal-optical methods. With the use of scanner and certain software, this research offers an easy, inexpensive way for higher school learners to assess and raise environmental consciousness on black carbon pollution in their surroundings. The research recommends that since digital imaging involves the controlled sampling parameters, the technique can be used as a sampling tool to estimate the EC concentrations when compared to the expensive instruments.

Jurányi et al., (2023) aims at determining the monthly variations in BC concentrations in the Arctic with particular focus on spring and summer. In spring and summer, obtained BC mass

concentrations are approximately four times higher, based on the data obtained from nine years of aircraft campaigns, equal to 21. The research also shows large fluctuations between years and regions specially during spring, while fair stability in summer. The fact that BC size distributions are fairly constant between seasons and the deviation of observed to modelled BC concentrations suggest that there is a requirement for enhanced modelling and additional analyses. The collected information allows to check the climate models and to gain deeper insight of influence of the region of British Columbia on the climate in the Arctic.

Du et al., (2011) states the Digital Optical Method for Black Carbon (DOM-BC) is newly devised and cost-effective approach for determination of BC concentrations in ambient aerosols with the help of digital photography. For this method, aerosol particles are deposited on quartz fiber filters that are then optically imaged and the optical attenuation (ATN) of the particle layer estimated. This ATN is related to BC mass loading through the calibration against the thermal–optical analysis (TOA). It was evidenced that ATN has a linear correlation with BC loading when ATN is less than 150 and an exponential correlation if ATN is greater than 200. It has been shown to possess a high degree of accuracy for the method deployed with less than ten relative error on average. It was found to be about 7% less accurate than TOA measurements, therefore offering practical advantages over conventional thermal and optical approaches as a result of its ease of use, speed, and cost effectiveness.

Wang et al., (2014) states the mixing state of refractory black carbon (rBC) aerosols and their implications for light absorption in Xi'an, China. The average rBC mass concentration was significantly higher during polluted periods compared to clean periods, with a substantial fraction of rBC internally mixed with other materials, enhancing light absorption. The research highlights that organics, sulfates, and nitrates are major contributors to the coatings on rBC particles, which significantly enhance their mass absorption cross-section. These findings emphasize the need for accurate measurements of rBC properties to improve climate models, particularly in regions with high particulate pollution.

CHAPTER 3

MATERIALS AND METHODS

3.1-Materials:

Selection of materials was one of the essential criteria to keep the security box functional, durable, and cost-efficient. The following materials were utilized in various components of the project:

No.	Name	Use
1.	RGB and IR Lights	Standardize the BC sample light for air monitoring purposes, providing of the pre- and post-filter light intensities.
2.	Arduino	Plays a core role in the system as the master processor of IOT, which processes the data from sensors, collects it, and communicates it among components.
3.	Liquid Crystal Display (LCD)	Offers an intuitive interface for displaying actual sensor results in real-time; this is so that users can easily keep tabs on the data and interpret it.
4.	Digital Humidity and Temperature sensor (DHT)	Being used for monitoring the environmental data such as temperature and humidity levels provides essential information for the atmospheric conditions.
5.	Global Positioning System (GPS)	It supplies precise locations data which allows for on-spot real-time geospatial mapping tracking and the user interface of the monitoring system.
6.	Particulate Matter Sensor (PMS) 5003	This tool collects PM2.5 particles in the air as they settle on a page, allowing the detection of air pollutants within the black carbon and other minute particles' category.
7.	Light Dependent Resistor (LDR)	Measure the variations in light intensity to acquire information for the level of BC concentration, which again comes from light absorption.
8.	Cables/ Connectors	Furnish the physical link and listening between the various elements of the monitoring system and thus, guarantee the harmonious workflow.
9.	Enclosure:	Protects essential components of the operating environment by being able to withstand dust, moisture, and corrosion, such as by decreasing potential for mechanical damage, thereby ensuring reliable performance in the field.
10.	Aethalometer	The aethalometer is a scientific instrument used to find black carbon particle concentration in the atmosphere. It is based on the light passing through a

		filter on which the particles have been deposited and detected by an attenuation process. Offers valuable insights for comparing the accuracy of black carbon concentrations with the black carbon detecting device.
--	--	--

Table 3.1.1

Device Workflow:

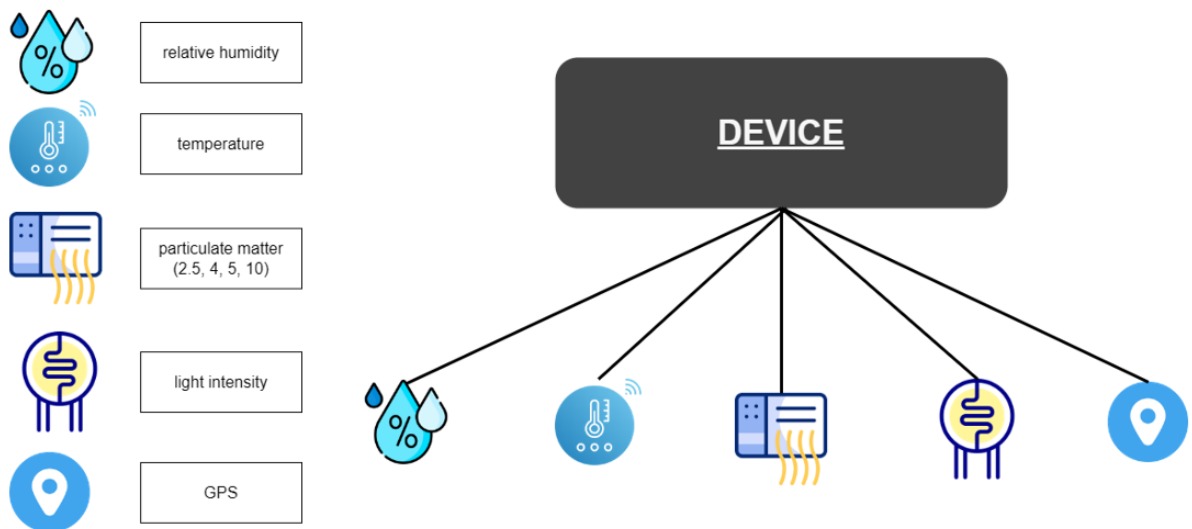


Figure 3.1 Materials and Equipment

The workflow shows that device measures relative humidity, temperature, concentration of particulate matter (2.5nm, 4nm, 5nm, 10nm), measures light intensity and Geographical data (latitude, longitude).

3.2-Methodology Flowchart:

The methodology flowchart is as under:

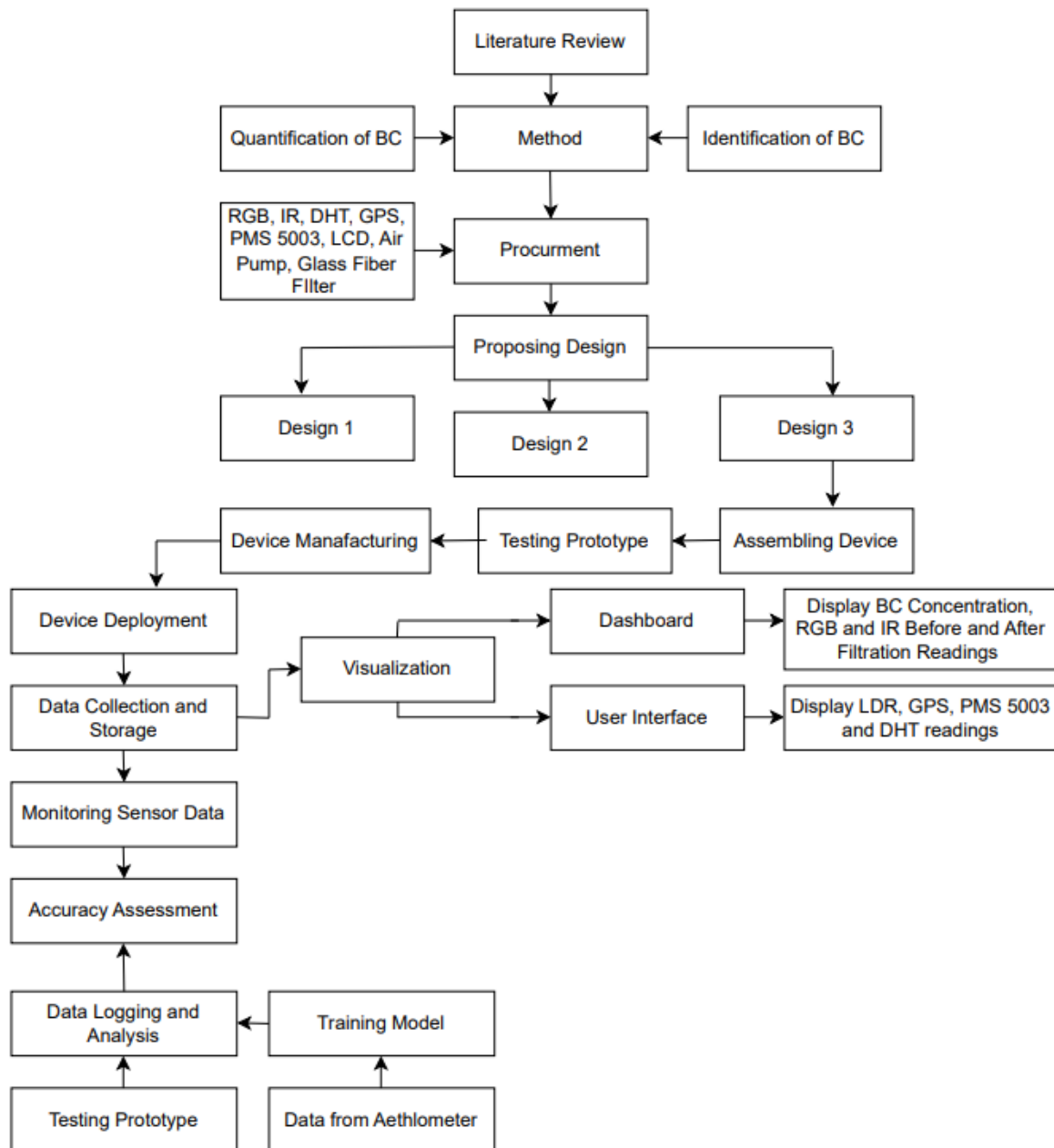


Figure 3.2 Methodological Framework

3.3-Methodology for ABCD:

In the device, a steady airflow is passed through the air pump to the structure of a tube. On both sides of the tube, RGB and IR LEDs are installed, along with Light Dependent Resistors (LDR) that are located directly opposite to it. Amid the core of the U-shaped tube built in, equipping the LED-LDR duo parts on both sides, a piece of the glass fiber filter paper is placed in the middle of the U-shaped device. The device is connected and powered by Arduino Nano, which is linked with a trifecta of sensors: the DHT sensor for humidity and temperature, the GPS sensor for finding latitude and longitude of study area, and the PMS sensor for finding

particulate matter (PM 2.5, 5, 7.5) concentrations in air. Finally, all these sensors' readings are displayed in a user-friendly interface created in python, and LCD display connected the Arduino Nano, ensuring that the data collected is readily accessible and comprehensible to the user.

The U-shaped device contains two chambers one before filtration and other after filtration. As the air from the atmosphere passes through the first chamber where one LDR records the RGB LEDs light intensities the other LDR records the IR LED light intensity, the air then passes through the glass fibre filter placed in the middle and moves to second chamber where each LDR records RGB and IR LED light intensities and finally the air is sucked by the air pump. The First chamber contains BC from the atmosphere and the second chamber contains clean air as the black carbon particles are filtered out, the light intensities are identified by the RGB and IR LEDs and compared to quantify the black carbon particles in the study area. As a result of presence of BC, the light is absorbed by the BC from the atmosphere so less light is detected by the LDR. LDR measures the intensity of light. The light intensity measured by IR LED is less in the presence of BC and more in the absence of BC after the air is filtered.

Data from each sensor is stored in excel and displayed through a Graphical User Interface (GUI) made in Python language. It helps users interact with the software application. The desired port of the PC is selected. start and stop buttons are displayed on the interface that records the values as start button is pressed and stores the values as soon as stop button is pressed. All the sensor data is shown by this GUI interface like the LEDs readings before and after filtration recorded by LDR sensor, GPS sensor reading showing exact Latitude and longitude of study area and DHT to find relative humidity and temperature. These readings help find what various factors have an impact on black carbon and exact location of black carbon particles. The data is saved in the excel file that can be viewed and monitored for any changes in sensor readings. From there data is visualized through a dashboard. The dashboard shows black carbon per minute concentrations which displays a graph that monitors the black carbon concentration that change with time in the study area and each LED readings recorded by LDR sensor that displays a statistical representation of before and after filtration readings of the LEDs. The LEDs readings show a considerable change before and after filtration of black carbon, especially IR LED as after filtration a constant trend is shown and per minute black carbon concentration of study area is displayed which gives valuable insights. The Data obtained is further used for creating study area map and heatmaps to show visual representation of the data points and the black carbon concentration data respectively.

For calculating the accuracy, the LED lights data obtained from LDR from before and after filtration of black carbon is compared with aethalometer black carbon data, the data collected from both devices is compared by using three different machine learning algorithms. The machine learning algorithms used are gradient boosting, random forest and XG boost. The R Square and Mean Absolute Percent Error is obtained from each machine learning algorithm and from that the accuracy can be found. The R square value for Gradient Boosting is 0.877, for Random Forest is 0.88 and for XG boost it shows 0.88. with this data it shows an accuracy of 94%. This device shows through a simple and cost-effective method black carbon particles can be detected, measured and mapped

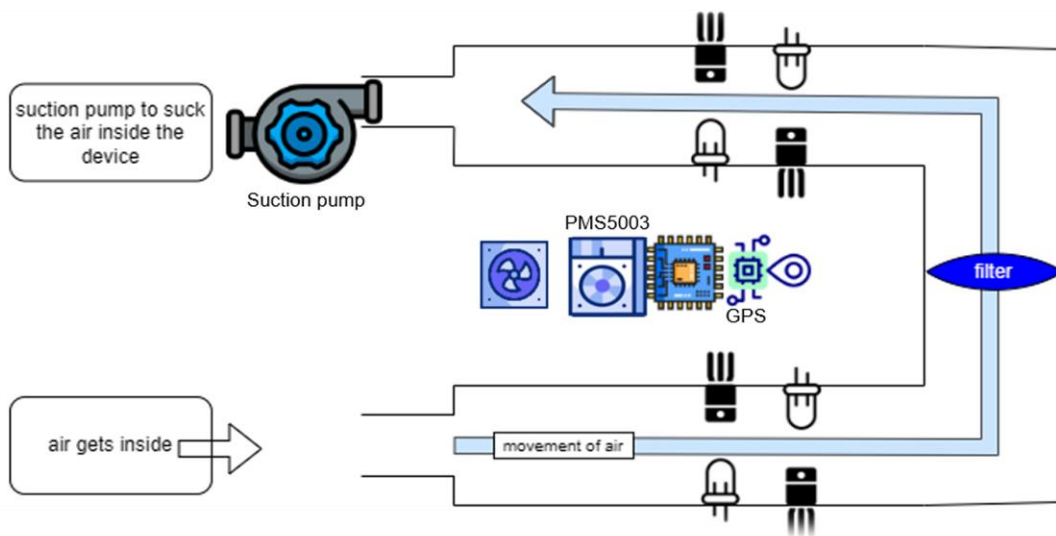


Figure 3.3 Shows Device Workflow

3.4 Equipment's

GPS

The GPS module is responsible for determining the location (latitude and longitude). The GPS module creates an instance of the TinyGPS class and define the readGPS() function to collect GPS data that listens to the serial port for GPS input data and parses it to obtain latitude and longitude values. If the data is valid, the job is updated; otherwise, the original value remains unchanged.

```

#include <TinyGPS.h>

TinyGPS gps; // Create a GPS object
float flat = 0.0; // Latitude
float flon = 0.0; // Longitude

void readGPS() {
    bool newData = false;
    for (unsigned long start = millis(); millis() - start < 1000;) {
        while (Serial.available()) {
            char c = Serial.read();
            if (gps.encode(c)) { // Checking if new valid sentence is received
                newData = true;
            }
        }
    }

    if (newData) {
        unsigned long age;
        gps.f_get_position(&flat, &flon, &age);
    }
}
}

```

Figure 3.5 shows Code Implementation of GPS

DHT 11

DHT11 sensor measures temperature and humidity. It connects to pin 10 and creates an instance of the SimpleDHT11 class. The readDHT11() function is defined to read the temperature and humidity and calculates the error to verify that the reading is accurate. If an error occurs, it sends the error code and time to the serial monitor.

```

#include <SimpleDHT.h>

int pinDHT11 = 10; // Pin used to connect DHT11 sensor
SimpleDHT11 dht11(pinDHT11); // Create a DHT11 object

byte temperature = 0; // Variable to store temperature
byte humidity = 0; // Variable to store humidity

void readDHT11() {
    int err = SimpleDHTErrSuccess;
    if ((err = dht11.read(&temperature, &humidity, NULL)) != SimpleDHTErrSuccess) {
        Serial.print("Read DHT11 failed, err=");
        Serial.print(SimpleDHTErrCode(err));
        Serial.print(",");
        Serial.println(SimpleDHTErrDuration(err));
        return;
    }
}
}

```

Figure 3.6 shows Code Implementation of DHT 11

LCD

LCD displays data from sensors with a 16x2 configuration, meaning it can display two columns of 16 characters each. The LCD, creates an object of the LiquidCrystal class and setupLCD() function initializes and displays the initialization message. The second function displayOnLCD(), makes text easier to display on the LCD by clearing the previous content and placing the new text on the specified line.

```
1  #include <LiquidCrystal.h>
2
3  const int rs = 4, en = 5, d4 = 6, d5 = 7, d6 = 8, d7 = 9; // LCD pin assignments
4  LiquidCrystal lcd(rs, en, d4, d5, d6, d7); // Create an LCD object
5
6  void setupLCD() {
7      lcd.begin(16, 2); // Initialize 16x2 LCD
8      lcd.print("System Start"); // Display startup message
9  }
10
11 void displayOnLCD(const String& line1, const String& line2) {
12     lcd.clear();
13     lcd.setCursor(0, 0);
14     lcd.print(line1); // First line
15     lcd.setCursor(0, 1);
16     lcd.print(line2); // Second line
17 }
```

Figure 3.7 shows Code Implementation of LCD

PMS 5003 Sensor

The PMS5003 sensor measures air quality, specifically particulate matter (PM) concentration. The SoftwareSerial function communicates with the sensor using pins 2 and 3 for RX and TX respectively. The pms5003data function stores sensor data. The readPMSdata() function reads data from the sensor, checks the number of bytes available, and checks the checksum to confirm that the data is correct. If valid, the data is stored in the specified format for further processing.

```

#include <SoftwareSerial.h>

SoftwareSerial pmsSerial(2, 3); // RX, TX for PMS5003 sensor
struct pms5003data {
  uint16_t framelen;
  uint16_t pm10_standard, pm25_standard, pm100_standard;
  uint16_t pm10_env, pm25_env, pm100_env;
  uint16_t particles_03um, particles_05um, particles_10um, particles_25um, particles_50um, particles_100um;
  uint16_t unused;
  uint16_t checksum;
};

pms5003data data; // Data structure to store PMS5003 data

boolean readPMSdata() {
  if (!pmsSerial.available()) {
    return false;
  }

  if (pmsSerial.peek() != 0x42) {
    pmsSerial.read();
    return false;
  }

  if (pmsSerial.available() < 32) {
    return false;
  }

  uint8_t buffer[32];
  uint16_t sum = 0;
  pmsSerial.readBytes(buffer, 32);

  for (uint8_t i = 0; i < 30; i++) {
    sum += buffer[i];
  }
}

```

Figure 3.8 shows Code Implementation of PMS 5003

```

  uint16_t buffer_u16[15];
  for (uint8_t i = 0; i < 15; i++) {
    buffer_u16[i] = buffer[2 + i * 2 + 1];
    buffer_u16[i] += (buffer[2 + i * 2] << 8);
  }

  memcpy((void *)&data, (void *)buffer_u16, 30);

  if (sum != data.checksum) {
    return false; // Checksum error
  }

  return true; // Success
}

```

Figure 3.9 shows Code Implementation of PMS 5003

Light Sensor Ambient (LUX)

LDR measures light intensity which initializes the variable to store red, green and blue readings and collects 500 samples to get a stable reading. The ReadLDR() function gives a measure of ambient light by calculating the average of these readings.

```
long ldr1_r = 0; // To measure red light
long ldr1_g = 0; // To measure green light
long ldr1_b = 0; // To measure blue light
long ldr2_r = 0; // Second set
long ldr2_g = 0;
long ldr2_b = 0;

void readLDR() {
    ldr1_r = 0;
    ldr1_g = 0;
    ldr1_b = 0;

    for (int a = 0; a <= 500; a++) {
        ldr1_r += analogRead(A7); // Red
        ldr1_g += analogRead(A4); // Green
        ldr1_b += analogRead(A7); // Blue
        delay(1);
    }

    ldr1_r /= 500;
    ldr1_g /= 500;
    ldr1_b /= 500;
}
```

Figure 3.10 shows Code Implementation of LDR

LEDs Light Emitting Diodes

LEDs are used as a visual display system. The pins of the red, green and blue LEDs are assigned in order. The setLEDs() function sets these pins as outputs and sets the initial state (blue LED on). The changeLED() function allows the status of each LED to change individually, providing visual feedback during system operation.

```

#define red 11 // Red LED
#define green 12 // Green LED
#define blue A0 // Blue LED

void setupLEDs() {
    pinMode(red, OUTPUT);
    pinMode(green, OUTPUT);
    pinMode(blue, OUTPUT);
    digitalWrite(red, 0); // Initially off
    digitalWrite(green, 0);
    digitalWrite(blue, 1); // Blue LED initially on
}

void changeLED(int redState, int greenState, int blueState) {
    digitalWrite(red, redState);
    digitalWrite(green, greenState);
    digitalWrite(blue, blueState);
}

```

Figure 3.11 shows Code Implementation of LEDs

3.5 Testing and Validation:

Sharma et al., (2017) estimated BC mass in three ways, none of which fully represent BC: transformation of light absorption determined with an Aethalometer for obtaining the equivalent black carbon (EBC), thermal desorption of the elemental carbon (EC) from the weekly integrated filter samples for obtaining the EC, and determination of the incandescence from the rBC part of the individual particles with the help of single particle soot photometer (SP2).

As there is no simple device to identify and quantify black carbon particles, so throughout the development of the black carbon detecting device, numerous versions were created with the primary goal of detecting and quantifying black carbon. Unfortunately, despite best efforts to produce reliable results, these designs did not prove accurate enough. The details of the design attempts are as follows:

First Design:

01

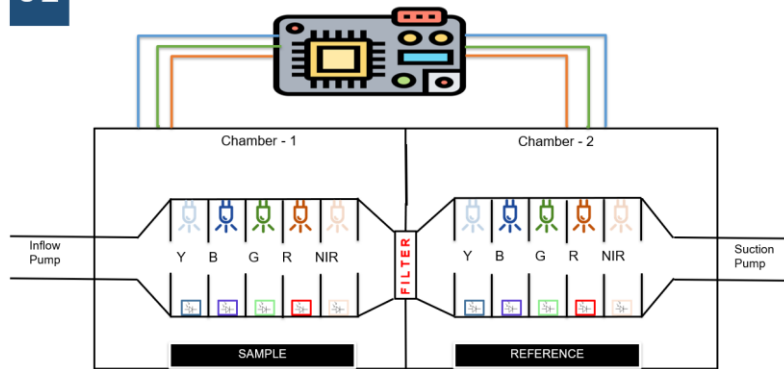


Figure 3.12 shows First Design

The device is designed in a straight chamber with an inlet pump that brings in air and passes it through a combination of RGB, yellow, and infrared light. The lighting isn't the end; LUX ambient sensors are present to quantify light usage. A filter is part of the device whose primary role is to capture carbon black (BC) depositing itself onto the filter paper. After filtration, BC-free air still goes through the light source plus sensor: Absence of BC would lead to less light absorption which shows that more light was received by the LUX Ambient sensor. This tells the mechanism because presence of BC causes absorption and reduces index value measured by LUX ambient sensor again. Adding on to this, device also has integrated an Arduino Nano into the mix, linking it up with a trifecta of sensors: DHT, GPS, and PMS sensor. And to tie it all together in a user-friendly interface to display data on LCD, ensuring that the data collected is readily accessible and comprehensible to the user. The light intensity measured by IR LED is less in the presence of BC and more in the absence of BC after the air is filtered. LDR measures the intensity of light. DHT sensor for humidity and temperature, GPS measures latitude and longitude. PMS5003 measures the concentration of BC particles (PM 2.5, 5, 7.5) in the atmosphere. Arduino nano is connected to LCD which displays intensities, temperature, humidity, PMS readings.

Data is displayed through a Graphical User Interface (GUI) made in Python language. It helps users interact with the software application. All the data of the sensors are shown by this GUI interface. The desired port of the PC is selected and start and stop buttons are displayed on the interface that records the values as start button is pressed and stores the values as soon as stop button is pressed. The data is saved in the excel file. From there data is visualized through a dashboard that displays black carbon concentrations and each LED intensity stored in LDR

sensors. Due to “Constructive Interference” between the LEDs the LUX readings were not accurate.

Second Design:

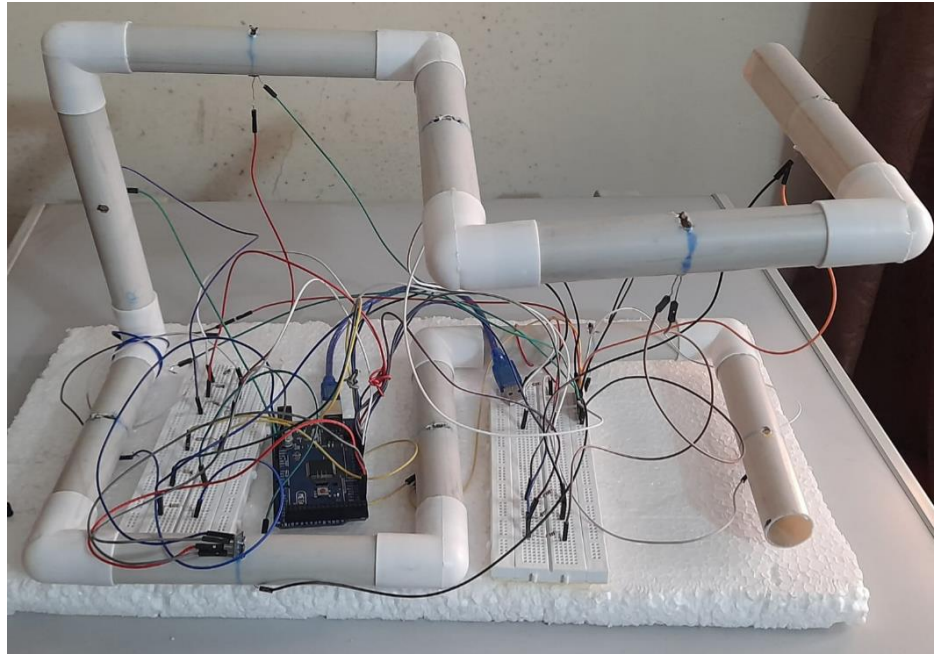


Figure 3.13 Shows Second Design

The next version of the tool is expected to have notable enhancements aimed at addressing “Constructive Interference” in the past and making it work better. Small pieces of tube on which LED is placed in the middle of the narrow tube. The diameter of the tube is 1cm. LUX sensors are placed opposite to LEDs.

Despite the efforts, these are further hindered by the large proportions and sensitivity of the system, but striving to be more effective by removing slits and having inputs in the corners still hampered by the cumbersome design due to the fact a small size leads to logistical problems – transportation after building and the installation and testing prove challenging; the system itself is highly sophisticated and so the process to manufacture it is highly complicated has it’s own large issues and is very complex; it also requires calibration or maintenance: thus large issues impacting flexibility with future designs and also the users point of view by just not making it easy enough. Adding on to this, this device also has integrated an Arduino Nano, linked with the same sensors as mentioned before DHT, GPS, and PMS sensor. LCD screen displays data and to monitor if readings are either correct or not, which tells intensities, location, temperature,

humidity, PMS readings especially PM 2.5 that help in quantifying the black carbon particles in air. The light intensity measured by IR LED is less in the presence of BC and more in the absence of BC after the air is filtered.

Graphical User Interface (GUI) displays the sensor data just like the previous design. The data is visualized through a dashboard that displays black carbon concentrations and each LED intensity stored in LDR sensors. The difference between the new design and previous design was the previous design kept a straight chamber for before and after filtration and the new design had more complex structure in order to counter the issue for constructive interference. Due to the same issue of “Constructive Interference” between the LEDs the LUX readings were not accurate and design was too complicated which led to the final design.

Final Design:

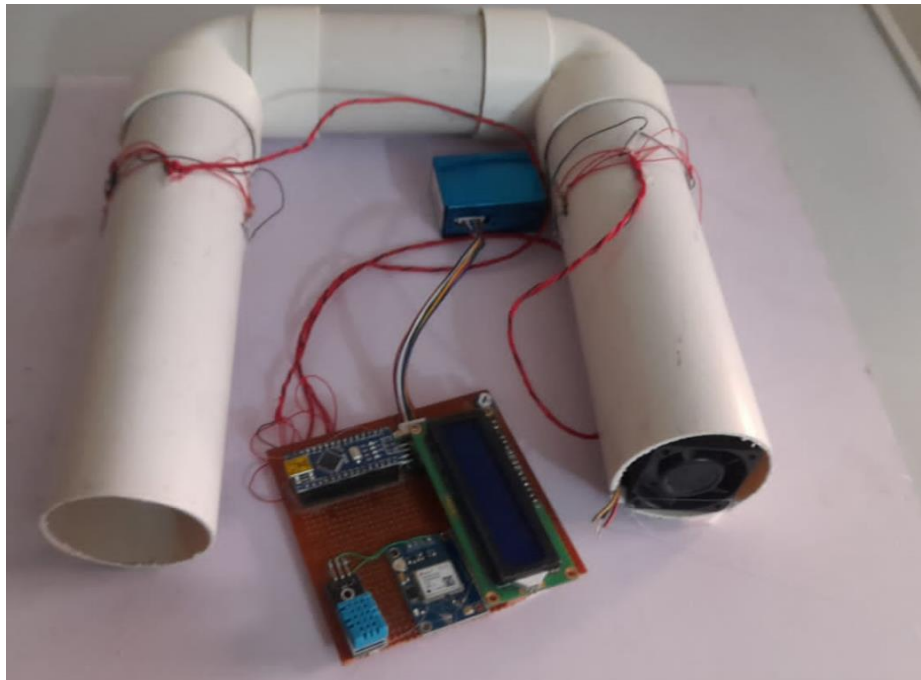


Figure 3.15 shows Final Design

The latest design of the black carbon detecting device resolves the major issues of Constructive interference and issue of size as the second design was too complex and difficult to carry from one place to another. This new design features a U-shaped configuration that minimizes all the errors like constructive interference, device design and improves performance. The basis of this work is the integration of RGB, and IR and opposite to it LDRs are used strategically to identify black carbon in the atmosphere. As air is drawn into the side of the U-shaped device, it passes through RGB and IR light sources, allowing carbon black to be detected. Importantly,

the fiberglass filter placed in the middle of the U-shaped device, making it easier for BC particles to be deposited onto the filter. Further, the filtered air flows through RGB and IR light sources that offer additional tools of light analysis and BC measurement. To improve the performance of the device and guarantee the acquisition and analysis of data in a timely manner, the Arduino Nano microcontroller is connected to the device with multiple sensors like DHT for relative humidity and temperature data, GPS for finding location data and PMS5003 sensors to help draw the PM2.5 particle concentration level. The outcomes are stored and presented on the LCD display and in form of dashboard to ensure the results are explained clearly. Thus, it is possible to say that all these characteristics form a comprehensive guide to detect the places measurement of black carbon in atmospheric.

Circuit design of the project:

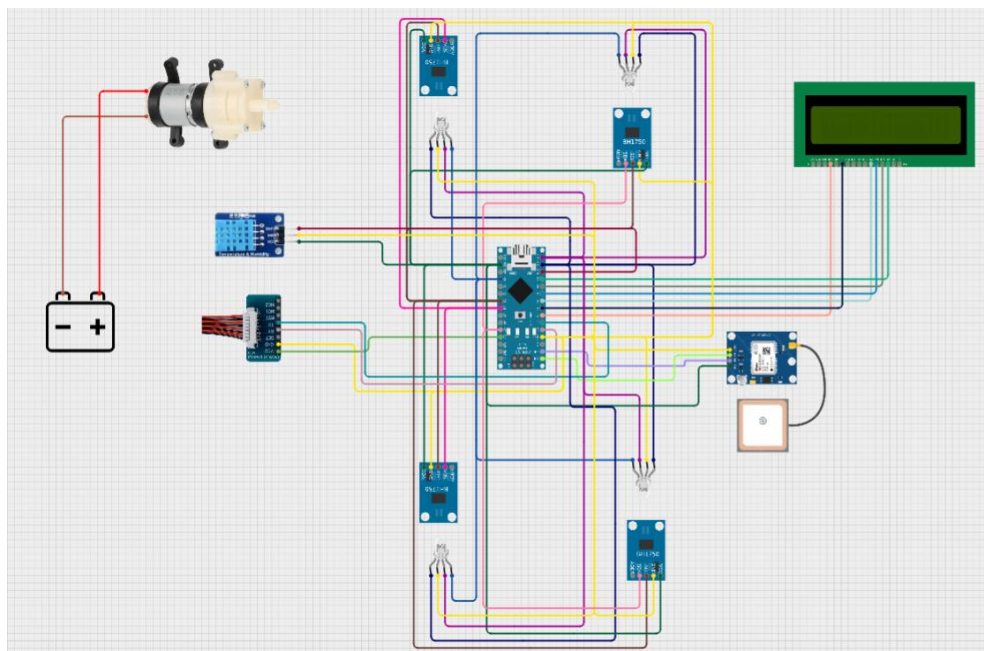


Figure 3.16 Circuit Diagram

It looks at why things didn't work well in the past. It shows how well this work can help people in future. It also puts research in bigger picture of growing knowledge and solving problems in the field.

RESULTS AND DISSCUSSION

4.1 Field Tests

The investigation into the proficiency of IoT machinery method was done through experimental trials. The deployment of devices in multiple areas facilitated the tracking of factors essential to BC levels, including air temperature, humidity, and light levels. The collected sensor data is stored in excel. The results are displayed on dashboard. Under various environmental conditions, the deployment and data collection process by observing the device mechanism during field tests yielded a considerable amount of data. By comparing the results with aethalometer and measuring the accuracy through machine learning algorithm, the accuracy of the device was found. The data that was collected from these tests thus played a key role in providing valuable ideas towards how the device could be made more effective in performance.

4.2 Device Mechanism Setup



Figure 4.1 shows complete Device setup with Aethalometer

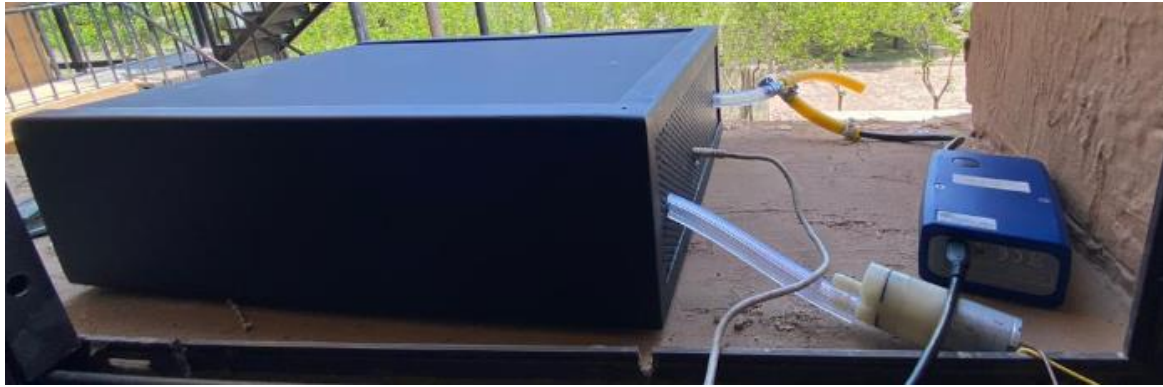


Figure 4.2 shows complete Device setup with Aethalometer

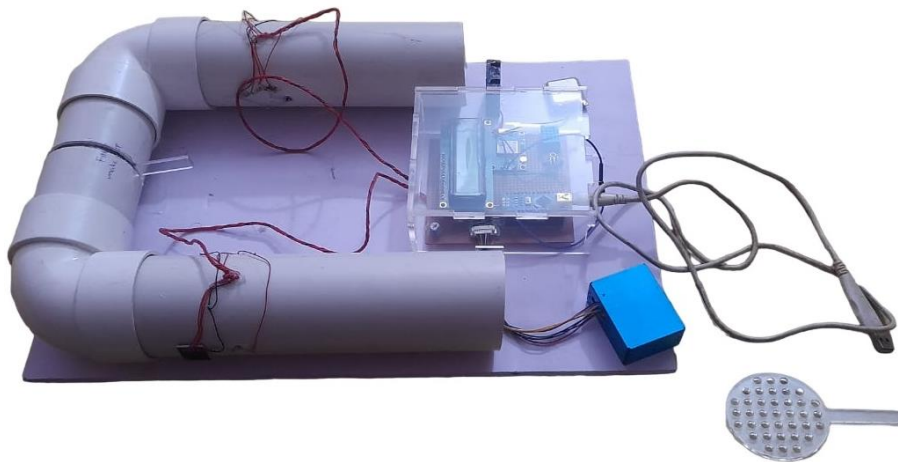


Figure 4.3 shows Device Internal Structure

4.3-Data Storage

The Data collected from device is stored in Excel format. The Data contains columns from Different RGD LEDs, and IR LEDs intensities recorded from light sensor, along with pm 2.5 concentration readings, temperature and humidity and location (Latitudes and Longitude).

RED_B	GREEN_B	BLUE_B	IR_B	RED_A	GREEN_A	BLUE_A	IR_A	.25w	.5W	.100W	Latitude	Longitude	Temp	Humidity	BC
651	823	834	24	600	788	786	1001	15	20	21	33.64814	72.98999	28	38	3787
654	826	835	24	608	791	788	1002	15	20	21	33.64814	72.98999	28	38	3688
654	826	835	24	608	791	788	1002	15	20	21	33.64814	72.98999	28	38	3704
654	826	835	24	608	791	788	1002	15	20	21	33.64814	72.98991	28	38	3572
655	830	843	24	614	805	806	1010	15	20	21	33.64814	72.98991	28	38	3671
655	830	843	24	614	805	806	1010	15	20	21	33.64814	72.98991	28	38	3581
655	830	843	24	614	805	806	1010	15	20	21	33.64814	72.98991	28	38	3526
653	821	831	23	606	786	783	999	15	20	21	33.64814	72.98991	28	38	3598
653	821	831	23	606	786	783	999	15	20	21	33.64814	72.98991	28	38	3426
653	821	831	23	606	786	783	999	15	20	21	33.64814	72.98991	28	38	3435
653	822	830	23	606	788	782	1000	15	20	21	33.64814	72.98991	28	38	3322
653	822	830	23	606	788	782	1000	15	20	21	33.64814	72.98991	28	39	3273
653	822	830	23	606	788	782	1000	15	20	21	33.64814	72.98993	28	39	3450
653	821	830	24	607	786	783	1000	15	20	21	33.64814	72.98993	28	39	3430
653	821	830	24	607	786	783	1000	15	20	21	33.64814	72.98993	28	39	3595
653	821	830	24	607	786	783	1000	15	20	21	33.64814	72.98994	28	39	4420
652	821	832	23	604	787	786	1008	15	20	21	33.64814	72.98994	28	39	3541
652	821	832	23	604	787	786	1008	15	20	21	33.64814	72.98994	28	38	3436
652	821	832	23	604	787	786	1008	15	20	21	33.64814	72.98994	28	38	3370
655	828	840	24	613	795	794	1006	15	20	21	33.64814	72.98994	28	38	3584
655	828	840	24	613	795	794	1006	15	20	21	33.64814	72.98994	28	38	3449
655	828	840	24	613	795	794	1006	15	20	21	33.64813	72.98994	28	38	3736
654	832	846	24	611	805	807	1006	15	20	21	33.64813	72.98994	28	38	3598
654	832	846	24	611	805	807	1006	15	20	21	33.64813	72.98994	29	38	3734
654	832	846	24	611	805	807	1006	15	20	21	33.64812	72.98994	29	38	3834

Figure 4.4 shows data in excel

4.4 Visualization

4.4.1 Dashboard

The dashboard created in Tableau for visualizing the device data like Red, Green, Blue and Infrared LEDs Intensities to help identify and quantify Black carbon particles. Display PMS Readings especially PM 2.5 Particles concentrations in air and measuring temperature and humidity of the study area. The Red, Green and Blue light show a significant change in values after filtration but IR shows a visible change as readings after BC is filtered shows a constant trend.

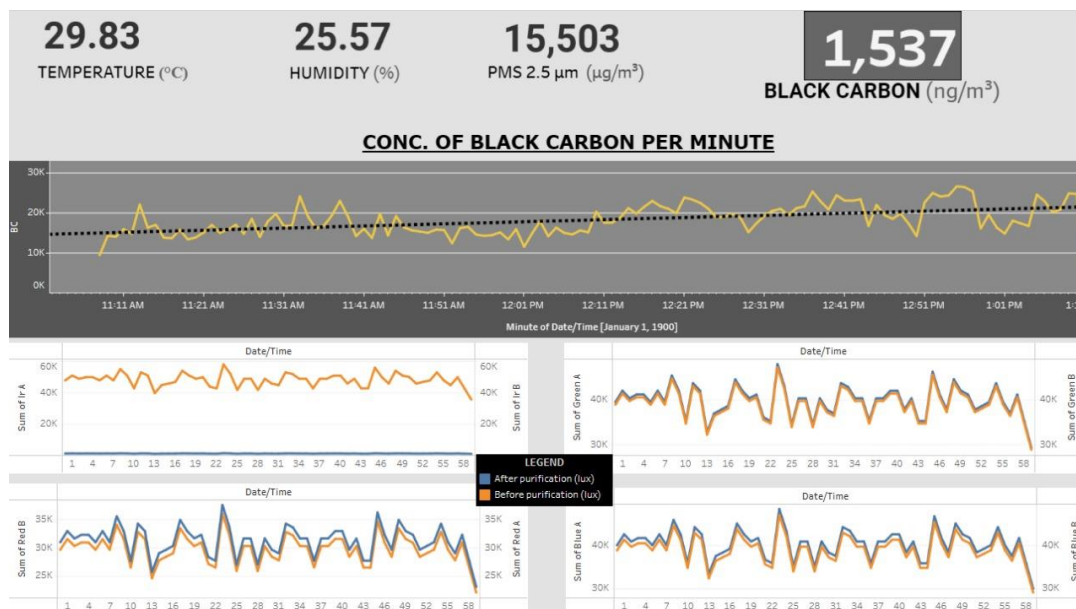


Figure 4.5 shows dashboard in tableau

4.4.2 Python GUI

The PMS 5003 Sensor, GPS, DHT, and LED readings are shown on the Python graphical user interface. When the device is connected to a PC, [python filename.py] command is entered, the start button is pressed, and the desired port is chosen to initiate the graphical user interface. LED readings for red, green, blue and IR are displayed, followed by PMS 5003 sensor, GPS, and DHT sensor readings.

The code used for graphical interface (GUI) built in Python using the PySide2 library, which is a Python language binding to the Qt framework. This code creates a large window with many

objects, allowing the user to interact with various widgets and communicate with the Arduino device via a network interface.

For initialization and adding global variables, the GUI imports various modules from PySide2 for GUI elements, layout controls, and other core functionality. It also imports many other libraries like serial, datetime and xlswriter. Many global variables are defined, including an Arduino serial connection source for creating a workbook and Excel files.

The main window (WidgetGallery) defines various layouts and sub window widgets. QStackedLayout is used to manage different "pages" in an application and allows switching between different views. The code creates three pages (P_2, P_3, and P_4) and defines various horizontal and vertical layouts for arranging widgets on these pages.

For creating various GUI elements, including buttons, labels, link boxes, and edit bars. GUI content is styled using a combination of font, size, colour, and background colour, usually using Times New Roman in a specific colour context. The main title tag uses a large font for visual appeal.

One of the pages (P_2) is designed for users to log in by entering their username and password. If the login password matches the predefined value ("Admin"), the GUI will proceed to the next page. This functionality is implemented by validating the click event handler of the button to enter the password.

In order to establish a serial connection to an Arduino device, the recurring timer function (recurring_timer) is set up to run periodically, reading data from the Arduino device. If valid data is received (denoted by a specific character, '#'), it is parsed and written to an Excel file. The data is also displayed on various line edits on the GUI, providing real-time feedback.

To manage GUI interactions, such as switching between pages, holding down buttons, and updating GUI elements. The Excel workbook is updated with the new data from the Arduino and the GUI will be updated with this data. This creates an interactive interface where users can view live data and control certain aspects of the application.

The main application loops and creates an instance of the WidgetGallery class and displays the GUI. The cycle continues until the user closes the application, allowing interaction and data processing to continue

```

from PySide2 import QtCore
from PySide2.QtCore import QDateTime, Qt, QTimer, QSize, QTime
from PySide2.QtCore import QTimer
from PySide2.QtGui import QPixmap
from PySide2.QtWidgets import (QApplication, QCheckBox, QComboBox, QDateTimeEdit,
    QDial, QDialog, QGridLayout, QGroupBox, QHBoxLayout, QLabel, QLineEdit,
    QProgressBar, QPushButton, QRadioButton, QScrollBar, QSizePolicy,
    QSlider, QSpinBox, QStyleFactory, QTableWidgetItem, QTabWidget, QTextEdit,
    QVBoxLayout, QWidget, QStackedLayout, QMainWindow, QScrollArea, QTimeEdit, QHeaderView, QComboBox, QMessageBox, QLineEdit)

from layout_1 import Color
import sys
import serial
import xlswriter
import datetime
now = datetime.datetime.now()
print (now.strftime("%Y-%m-%d %H:%M:%S"))
global row
row=1
global arduino
arduino=0
filename_=now.strftime("%Y_%m_%d_%H_%M_%S")+ ".xlsx"
header = (
    ['Date/Time'],
    ['RED_B'],
    ['GREEN_B'],
    ['BLUE_B'],
    ['IR_B'],
    ['RED_A',1],
    ['GREEN_A'],
    ['BLUE_A'],
    ['IR_A'],
    ['.25w'],
    ['.5W'],
    ['.100W'],
    ['Latitude'],
    ['Longitude'],
    ['Temp'],
    ['Humidity'],
)

workbook = xlswriter.Workbook(filename_)
worksheet = workbook.add_worksheet()
col=0
for items in (header):
    #print()
    worksheet.write(0, col,items[0])
    col=col+1

```

Figure 4.6 shows code implementation of GUI Interface in python

4.4.3 Study Area

The study area map is created using ArcGIS software. The Excel data obtained from the black carbon detecting device deployed in the study area. The data contains Latitude and longitude which can be imported in Arc GIS as XY point data. The projection is set to (WGS 1984).

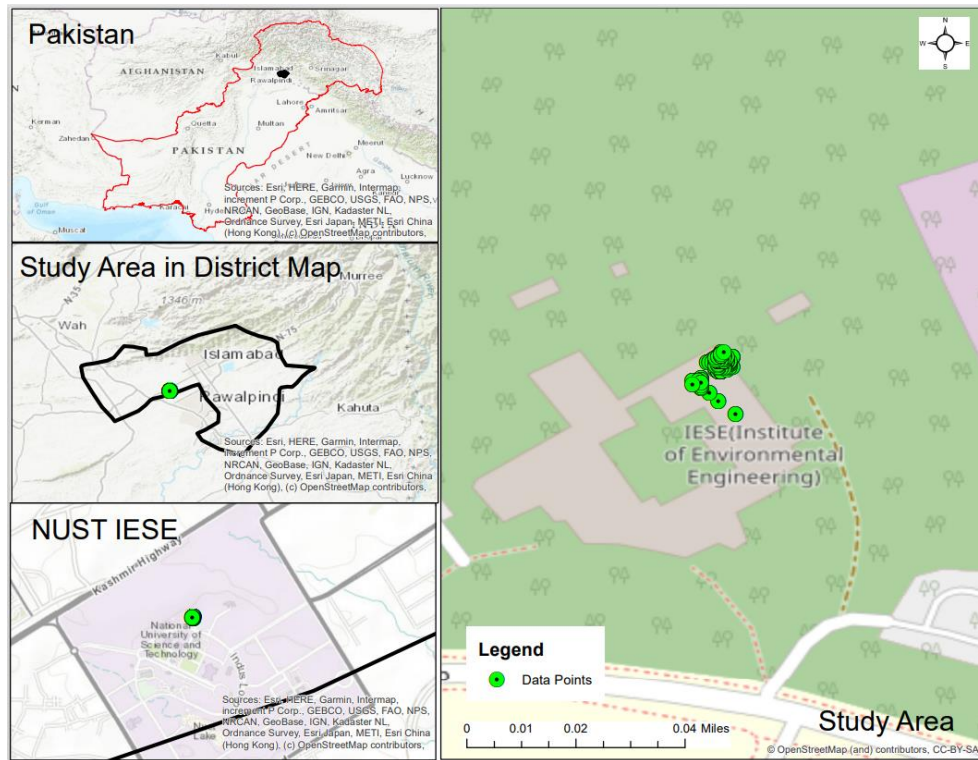


Figure 4.9 Shows Study Area

4.4.4 Heatmaps

Heatmaps of the data created using ArcGIS Pro. The excel data imported in ArcGIS pro as XY point data. The X Field is kept as Longitude, Y Field is kept as Latitude and desired Projection system is set (WGS 1984).

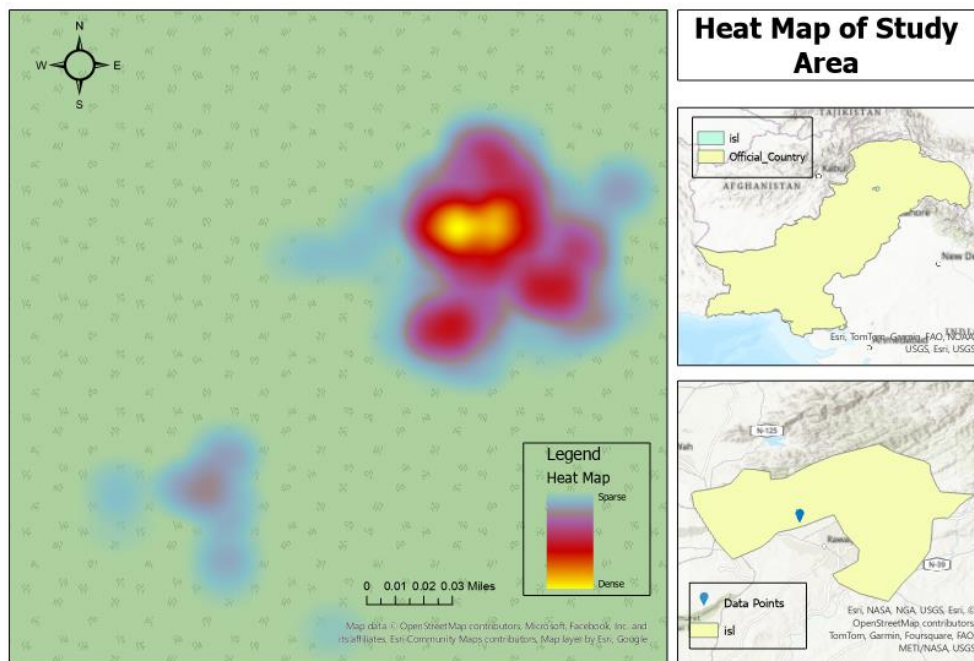


Figure 4.10 shows Heat Maps of the Study Area

4.5 Accuracy Assessment and Validation

Sajjadi et al., (2017) assessed PM2.5 and PM10 concentrations by using three different interpolation models and comparing the MAPE (Mean Absolut Percent Error) values to determine the most accurate interpolation method.

For this research through python, R Square and MAPE values are compared by using three different machine learning models. In order to approach this firstly, data processing step requires essential core libraries: Pandas, Numpy, and Seaborn which are used for data manipulation and visualization and various Scikit-Learn modules for machine learning, second step data scaling, and model. The SimpleImputer class which fills any missing items in the configuration file with the meaning of the corresponding string as it guarantees that the dataset is ready for further analysis without any issues due to missed files. The target variable “BC” meaning black carbon. Additionally, splits the data into training and testing steps: the 80-20 split ratio and a random seed retraining element are used.

Data scaling an important step because it brings all the features required for many machine learning algorithms to a similar level. Use the same scaling method for different purposes for consistency.

Finally, three machine learning algorithms are used for finding the accuracy, the three models are gradient boosting, random forest and XG Boost.

Gradient Boosting

Gradient boosting is a machine learning technique for regression and classification problems that produces a prediction model in the form of an ensemble of weak prediction models, typically decision trees. The GridSearchCV function and a set of hyperparameters, then linear search method is adjusted accordingly to find the most optimal configuration for the model. These are the best parameters that can be the predictors number, a training value, and the minimum value that will optimize the model. Furthermore, the linear search method with 5 cross-validations is the best method to predict the performance model. Thus, the training model makes predictions in testing. Then predicted the values obtained, and are converted to the original values for evaluation.

For measuring the performance of the gradient boosting regressor R Squared value and Mean Absolute Percent error are evaluated. This measurement includes:

- **R-squared:** which shows the proportion of variation explained by the model. The value nearer to 1 indicates a better fit.
- **Mean Absolute Percent Error:** calculates the percentage error which indicates on average how close or far off the top model prediction is from the true value.

```
# Invert scaling for predicted values
y_test_pred_orig_scale = scaler_y.inverse_transform(np.expand_dims(y_test_pred, axis=1)).squeeze()

# Calculate additional metrics
mse = mean_squared_error(y_test, y_test_pred_orig_scale)
rmse = np.sqrt(mse)
r2 = r2_score(y_test, y_test_pred_orig_scale)
mae = mean_absolute_error(y_test, y_test_pred_orig_scale)
mape = mean_absolute_percentage_error(y_test, y_test_pred_orig_scale)

# Fit a linear regression model for best-fit line
linear_regression = LinearRegression()
linear_regression.fit(np.expand_dims(y_test, axis=1), y_test_pred_orig_scale)

# Best-fit line equation
slope = linear_regression.coef_[0]
intercept = linear_regression.intercept_

best_fit_line = f"y = {slope:.2f}x + {intercept:.2f}"

# Display additional results
print("Best Hyperparameters for Gradient Boosting:", best_params_gb)
print(f"Gradient Boosting Mean Squared Error (Test): {mse}")
print(f"Gradient Boosting Root Mean Squared Error (Test): {rmse}")
print(f"Gradient Boosting R-squared (Test): {r2}")
print(f"Gradient Boosting Mean Absolute Error (Test): {mae}")
print(f"Mean Absolute Percentage Error (Test): {mape}")
print("Equation for Best-Fit Line:", best_fit_line)

# Create scatter plot with best-fit line
x_range = np.linspace(y_test.min(), y_test.max(), 100)
y_range = slope * x_range + intercept
```

Figure 4.11 Code Implementation for Data Training and Accuracy Assessment

```
plt.figure(figsize=(8, 6))
sns.scatterplot(x=y_test, y=y_test_pred_orig_scale, label='Data Points')

# Plot the best-fit Line
plt.plot(x_range, y_range, color='red', label='Best-Fit Line')

# Customize the plot
plt.xlabel('Actual (BC)')
plt.ylabel('Predicted (BC)')
plt.title('Actual vs Predicted Black Carbon with Best-Fit Line')
plt.legend()
plt.show()
```

Figure 4.12 Code Implementation for Data Training and Accuracy Assessment Figure

Gradient Boosting R-squared (Test): 0.877

Mean Absolute Percentage Error (Test): 12.57

Equation for Best-Fit Line: $y = 0.97x + 160.45$

Figure 4.13 Results for Gradient Boosting Algorithm

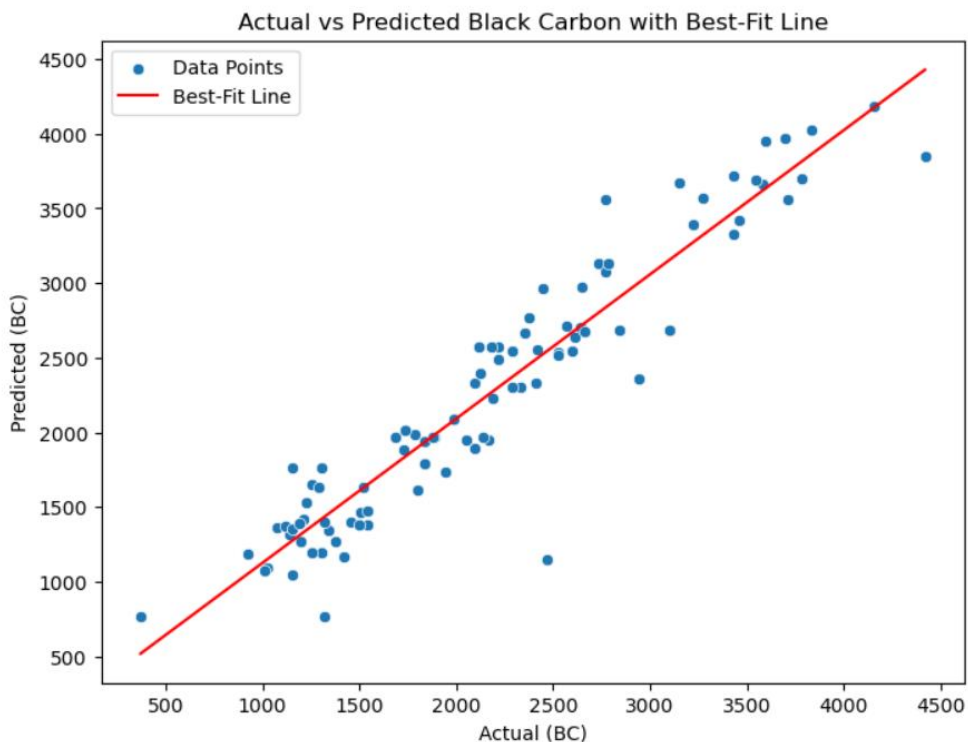


Figure 4.14 shows best fit line graph

Random Forest

A machine learning model Random Forest is a robust ensemble learning method that builds multiple decision trees and combines them to improve model accuracy and prevent overfitting. GridSearchCV, which searches for the best hyperparameters of the random forest, develops the model. Grid parameters include:

- Number of predictors (trees in the forest).
- Maximum depth of each tree.
- Minimum samples required to split a node and minimum samples required at a leaf.

GridSearchCV uses 5-fold cross-validation to ensure stability of settings. When visibility is detected to be poor, the model is trained using these suggestions. The training model is then used to make predictions for testing. Since the material was calibrated, the predicted values were converted to the original scale for evaluation.

For measuring the performance of the Random Forest, the R Squared value and Mean Absolute Percent error values are evaluated. This measurement includes:

- **R-squared:** which shows the proportion of variation explained by the model. The value nearer to 1 indicates a better fit.
- **Mean Absolute Percent Error:** is utilized to calculate the percentage error which indicates on average how close or far off the top model prediction is from the true value.

The results show the model performance on the parameter by extracting the optimal hyperparameters of the Random Forest regressor and all parameter values. The equation of the best line showing the relationship between actual and predicted values. The figure 4.18 shows values on the x-axis and estimated values on the y-axis. Red line representing the line of best fit is also added to the graph to indicate the difference which provides a visual representation of the model's accuracy and predictive power.

```

# Invert scaling for predicted values
y_test_pred_orig_scale = scaler_y.inverse_transform(y_test_pred.reshape(-1, 1)).squeeze()

# Calculate evaluation metrics
mse = mean_squared_error(y_test, y_test_pred_orig_scale)
rmse = np.sqrt(mse)
r2 = r2_score(y_test, y_test_pred_orig_scale)
mae = mean_absolute_error(y_test, y_test_pred_orig_scale)
mape = mean_absolute_percentage_error(y_test, y_test_pred_orig_scale)

# Fit a linear regression model for best-fit line
linear_regression = LinearRegression()
linear_regression.fit(np.expand_dims(y_test, axis=1), y_test_pred_orig_scale)

# Best-fit line equation
slope = linear_regression.coef_[0]
intercept = linear_regression.intercept_

best_fit_line = f"y = {slope:.2f}x + {intercept:.2f}"

# Display additional results
print("Best Hyperparameters for Random Forest:", best_params_rf)
print(f"Random Forest Mean Squared Error (Test): {mse}")
print(f"Random Forest Root Mean Squared Error (Test): {rmse}")
print(f"Random Forest R-squared (Test): {r2}")
print(f"Random Forest Mean Absolute Error (Test): {mae}")
print(f"Mean Absolute Percentage Error (Test): {mape}")
print("Equation for Best-Fit Line:", best_fit_line)

# Create scatter plot with best-fit line
x_range = np.linspace(y_test.min(), y_test.max(), 100)
y_range = slope * x_range + intercept

```

Figure 4.15 Code Implementation for Data Training and Accuracy Assessment

```

plt.figure(figsize=(8, 6))
sns.scatterplot(x=y_test, y=y_test_pred_orig_scale, label='Data Points')

# Plot the best-fit line
plt.plot(x_range, y_range, color='red', label='Best-Fit Line')

# Customize the plot
plt.xlabel('Actual (BC)')
plt.ylabel('Predicted (BC)')
plt.title('Actual vs Predicted Black Carbon with Best-Fit Line')
plt.legend()
plt.show()

```

Figure 4.16 Code Implementation for Data Training and Accuracy Assessment

Random Forest R-squared (Test): 0.88

Mean Absolute Percentage Error (Test): 12.23

Equation for Best-Fit Line: $y = 0.94x + 195.21$

Figure 4.17 Results for Random Forest Algorithm

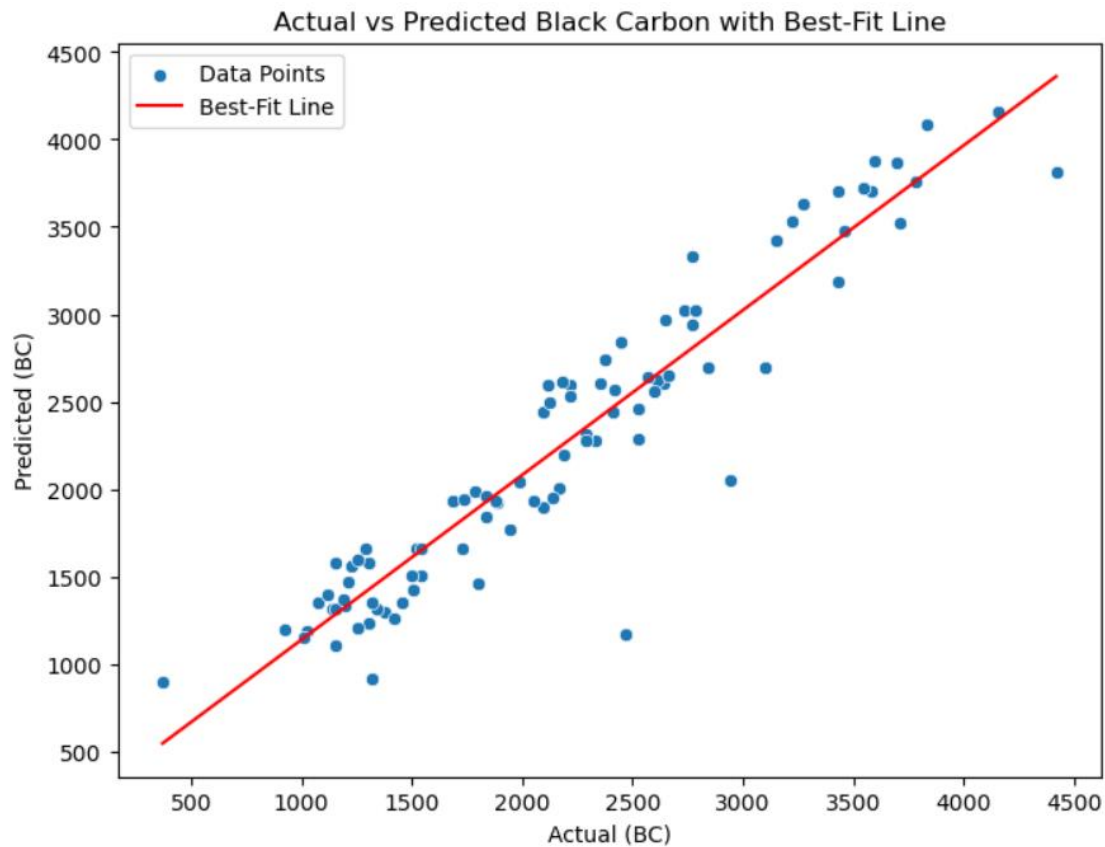


Figure 4.18 shows best fit line graph

XG Boost Algorithm

XG Boost Regressor is a machine learning model. XG Boost is a powerful learning algorithm that combines multiple weak learners to create robust predictive models. To optimize the model, grid conditions are defined for GridSearchCV, which searches for the best hyperparameters. Grid parameters include:

Number of predictors (trees in the forest). To find the best parameter configuration. This process allows a good evaluation of the model's performance and ensures that the options are not bad. When a negative view is found, the XG Boost model automatically reuses these views.

The training model is then used to make predictions for testing. For evaluation, change the estimated value back to the original scale.

For measuring the performance of the Random Forest, the R Squared value and Mean Absolute Percent error values are evaluated. This measurement includes:

- **R-squared:** which shows the proportion of variation explained by the model. The value nearer to 1 indicates a better fit.
- **Mean Absolute Percent Error:** is utilized to calculate the percentage error which indicates on average how close or far off the top model prediction is from the true value.

The results show the model performance on the parameter by extracting the optimal hyperparameters of the XG Boost regressor and all parameter values. It also shows the equation of the best line showing the relationship between actual and predicted values. The figure 4.22 shows values on the x-axis and estimated values on the y-axis. Red line representing the line of best fit is also added to the graph to indicate the difference which provides a visual representation of the model's accuracy and predictive power.

```
# Invert scaling for predicted values
y_test_pred_orig_scale = scaler_y.inverse_transform(y_test_pred.reshape(-1, 1)).squeeze()

# Calculate evaluation metrics
mse = mean_squared_error(y_test, y_test_pred_orig_scale)
rmse = np.sqrt(mse)
r2 = r2_score(y_test, y_test_pred_orig_scale)
mae = mean_absolute_error(y_test, y_test_pred_orig_scale)
mape = mean_absolute_percentage_error(y_test, y_test_pred_orig_scale)

# Fit a linear regression model for best-fit line
y_test_array = y_test.to_numpy().reshape(-1, 1) # Fix for reshape error
linear_regression = LinearRegression()
linear_regression.fit(y_test_array, y_test_pred_orig_scale)

# Best-fit line equation
slope = linear_regression.coef_[0]
intercept = linear_regression.intercept_

best_fit_line = f"y = {slope:.2f}x + {intercept:.2f}"

# Display additional results
print("Best Hyperparameters for XGBoost:", best_params_xgb)
print(f"XGBoost Mean Squared Error (Test): {mse}")
print(f"XGBoost Root Mean Squared Error (Test): {rmse}")
print(f"XGBoost R-squared (Test): {r2}")
print(f"XGBoost Mean Absolute Error (Test): {mae}")
print(f"Mean Absolute Percentage Error (Test): {mape}")
print("Equation for Best-Fit Line:", best_fit_line)

# Create scatter plot with best-fit line
x_range = np.linspace(y_test.min(), y_test.max(), 100)
y_range = slope * x_range + intercept
```


Figure 4.19 Code Implementation for Data Training and Accuracy Assessment

```
plt.figure(figsize=(8, 6))|
sns.scatterplot(x=y_test, y=y_test_pred_orig_scale, label='Data Points')

# Plot the best-fit line
plt.plot(x_range, y_range, color='red', label='Best-Fit Line')

# Customize the plot
plt.xlabel('Actual (BC)')
plt.ylabel('Predicted (BC)')
plt.title('Actual vs Predicted Black Carbon with Best-Fit Line')
plt.legend()
plt.show()
```

Figure 4.20 Code Implementation for Data Training and Accuracy Assessment

XGBoost R-squared (Test): 0.88

Mean Absolute Percentage Error (Test): 12.13

Equation for Best-Fit Line: $y = 0.95x + 167.19$

Figure 4.21 Results for XG Boost Algorithm

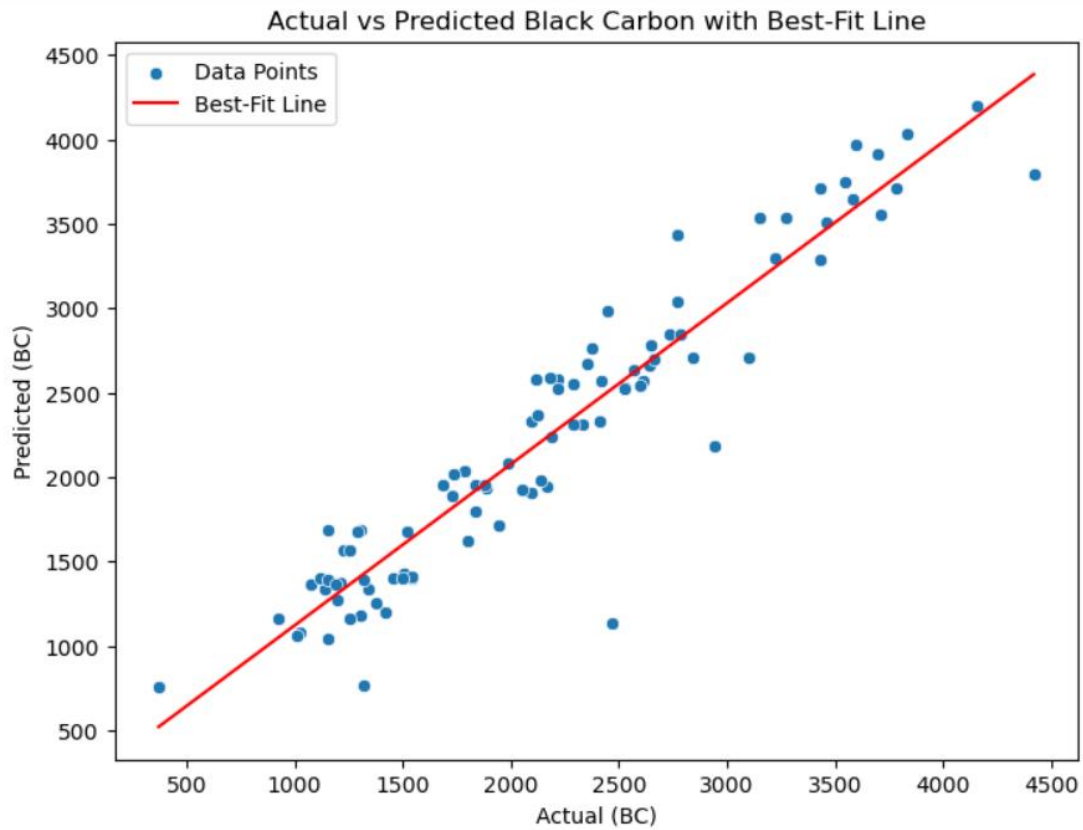


Figure 4.22 shows best fit line graph

The validation of data is conducted by observing the data from the device with aethalometer for 2 days and data from aethalometer is combined with data collected from the device, further machine learning algorithms are used to check accuracy of device with Aethalometer. The machine learning models used are gradient boosting, random forest and XG Boost which shows R square value of 0.877, 0.88 and 0.88 respectively. When the R square and Mean Absolute Percent Error are compared for the three machine learning algorithms it shows an accuracy of 94%. This accuracy shows the data collected from the black carbon detecting device is accurate and reliable for future use, this device shows through a simple and cost-effective method black carbon particles in the air can easily be identified, quantified and mapped.

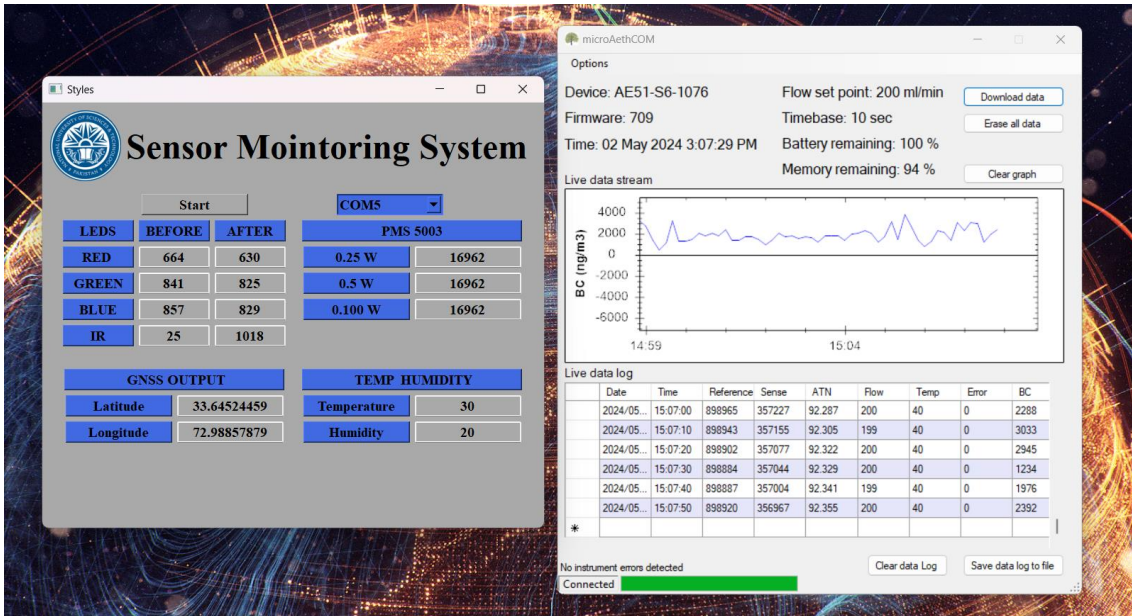


Figure 4.23 shows Validation of data by observing and combining data from aethalometer and from black carbon detecting device

CHAPTER 5

CONCLUSION

The study aims to analyse the fusion of cutting-edge technology with innovative design has given birth to a high-tech air quality surveillance setup. The device employs RGB and infrared LEDs with Light Dependent Resistors (LDR) as well as DHT sensor for temperature and humidity, GPS for geographical data, PMS5003 sensor for particulate matter concentration in our system, aiming to ensure no aspect is left unmonitored. The capacity to log and save information in Excel format allows for additional examination and understandings into air quality patterns as time passes. At last, this framework gives a significant device for people and associations that try to screen and reduce the effect of air contamination on wellbeing and prosperity. Its flexibility and simplicity of use enable clients to settle on educated choices and make proactive moves to address air quality concerns in their environmental factors. Thus, this device aims to introduce a simple and cost-effective method to identify, quantify and map black carbon particles in the air.

BENEFICIARIES

Explain the beneficiaries of the project, how various stakeholders including the following stand to gain from its outcome.

1. Ministry of Climate Change:

Coordinates, monitoring and implementation of environmental agreements with other countries, internal agencies and forums. As black carbon contributes to warming by being very effective at absorbing light the black carbon detecting device helps take proactive measures and improve air quality.



2. Sustainable Development Policy Institute

The sustainable development policy institute is a non-profit research organization based in Islamabad, Pakistan. It was founded in 1992 with the goal of sustainable development in Pakistan and wider South Asian Region through research, policy analysis and advocacy. The black carbon device can help researcher to help create awareness about the dangers of black carbon in atmosphere.



3. World Health Organization

WHO works worldwide to promote health, keep the world safe and serve the vulnerable. Black carbon contributes to climate change and ill health. WHO have recognized black carbon as a key pollutant in causing heart problems, respiratory diseases and premature death. The black carbon detecting device can help identify sources of black carbon and monitor the progress to establish new policies.



4. Climate/Air Quality Researchers

It helps climate and air quality researchers in their study and further research. The black carbon device can help researcher to get a better understanding of black carbon and its impact on climate and human health, and help get accurate measurement of black carbon concentrations in air to gain valuable insights.



RECCOMENDATION

1. **Sensor Optimization:** Research should concentrate on optimizing the sensors especially for sensing black carbon aerosols in the environment. Research should focus on enhancing the capability of these sensors in regard to sensitivity and specificity to black carbon.
2. **Miniaturization:** Efforts should be made to minimize the size and mass of the device while at the same time improving, or at least preserving the accuracy of BC measurement and differentiation. It may require the employment of certain specific materials and structural forging approaches which is well adjusted for black carbon identification.
3. **AI Integration:** Requires incorporation of new AI algorithms which have been specifically designed to make analysis of black carbon data. It is possible to design these AI engines for improving the real-time active monitoring of the detector; to perform an anomaly check on black carbon levels; and to self-calibrate the ‘smart’ sensors based on changing environmental characteristics.
4. **Data Fusion:** Introduce a data fusion approach used to integrate data received from different sensors intended for the black carbon and other similar particulates detection. Thus, the impact of this approach can result in the improved identification and assessment of the environmental conditions with reference to black carbon pollution.
5. **Energy Efficiency for Prolonged Black Carbon Monitoring:** Creating power management policies relevant to the running of black carbon detection devices. More effort should be directed on conserving energy so as to serve the field conditions where such a device may be required to run for a very long time.
6. **Collaborative Development:** Consult with professionals in environmental science and public health so that the device suits the needs of black carbon measurement in different settings. It can lead the enhancement process to cope up with the problems of black carbon and its manifestation with respect to health and environment.

REFERENCES

1. Bahadur, R., Praveen, P.S., Xu, Y., Ramanathan, V., 2012. Solar absorption by elemental and brown carbon determined from spectral observations. *Proc. Natl. Acad. Sci.* 109, 17366–17371.
<https://doi.org/10.1073/pnas.1205910109>
2. Cheng, J.Y.W., Chan, C.K., Lau, A.P.S., 2011. Quantification of airborne elemental carbon by digital imaging. *Aerosol Sci. Technol.* 45, 581–586.
<https://doi.org/10.1080/02786826.2010.550960>
3. Du, K., Wang, Y., Chen, B., Wang, K., Chen, J.S., Zhang, F.W., 2011. Digital photographic method to quantify black carbon in ambient aerosols. *Atmos. Environ.* 45, 7113–7120.
<https://doi.org/10.1016/j.atmosenv.2011.09.035>
4. Wang, Q., Huang, R.J., Cao, J., Han, Y., Wang, G., Li, G., et al., 2014. Mixing state of black carbon aerosol in a heavily polluted urban area of China: implications for light absorption enhancement. *Aerosol Sci. Technol.* 48, 689–697.
<https://doi.org/10.1080/02786826.2014.917758>
5. Jurányi, Zsófia & Zanatta, Marco & Lund, Marianne & Samset, Bjørn H. & Skeie, Ragnhild & Sharma, Sangeeta & Wendisch, Manfred & Herber, Andreas. (2023). Atmospheric concentrations of black carbon are substantially higher in spring than summer in the Arctic. *Communications Earth & Environment*. 4. 10.1038/s43247-023-00749-x.
<https://doi.org/10.1038/s43247-023-00749-x>
6. Caubel, Julien & Cados, Troy & Kirchstetter, Thomas. (2018). A New Black Carbon Sensor for Dense Air Quality Monitoring Networks. *Sensors*. 18. 738. 10.3390/s18030738.
<https://doi.org/10.3390/s18030738>
7. Sharma, Sangeeta & Leitch, W. & Huang, L. & Veber, Dan & Kolonjari, Felicia & Zhang, Wendy & Hanna, Sarah & Bertram, Allan & Ogren, John. (2017). An Evaluation of three methods for measuring black carbon at Alert, Canada. *Atmospheric Chemistry and Physics Discussions*. 17. 1-42. 10.5194/acp-17-15225-2017.
<https://doi.org/10.5194/acp-17-15225-2017>
8. Michael R. Olson, Eric Graham, Samera Hamad, Pajeau Uchupalanun, Nithya Ramanathan, James J. Schauer (2016) Quantification of elemental and organic carbon in atmospheric particulate matter using color space sensing—hue, saturation, and value (HSV) coordinates *Science of The Total Environment*, Volumes 548–549, Pages 252-259, ISSN 0048-9697.

<https://doi.org/10.1016/j.scitotenv.2016.01.032>

9. Krämer, L., Bozoki, Z., & Niessner, R. (2002). Characterisation of a mobile photoacoustic sensor for atmospheric black carbon monitoring. *Analytical Sciences/Supplements*, 17(0), s563-s566.
<https://doi.org/10.14891/analscisp.17icpp.0.s563.0>
10. Petzold, A., & Schönlinner, M. (2004). Multi-angle absorption photometry—a new method for the measurement of aerosol light absorption and atmospheric black carbon. *Journal of Aerosol Science*, 35(4), 421-441.
<https://doi.org/10.1016/j.jaerosci.2003.09.005>
11. Highwood, E. J., & Kinnersley, R. P. (2006). When smoke gets in our eyes: The multiple impacts of atmospheric black carbon on climate, air quality and health. *Environment international*, 32(4), 560-566.
<https://doi.org/10.1016/j.envint.2005.12.003>
12. Caubel, J. J., Cados, T. E., Preble, C. V., & Kirchstetter, T. W. (2019). A distributed network of 100 black carbon sensors for 100 days of air quality monitoring in West Oakland, California. *Environmental science & technology*, 53(13), 7564-7573.
<https://doi.org/10.1021/acs.est.9b00282>
13. Sajjadi, S. A., Zolfaghari, G., Adab, H., Allahabadi, A., & Delsouz, M. (2017). Measurement and modeling of particulate matter concentrations: Applying spatial analysis and regression techniques to assess air quality. *MethodsX*, 4, 372-390.
<https://doi.org/10.1016/j.mex.2017.09.006>

Appendix

Expenditure for Device

Vendor	Equipment	Qautntity	Prices
Electrobes	GPS Module	1	PKR 1,000.00
Electrobes	DHT-11	1	PKR 220.00
DigiLog	LUX sensor	10	PKR 6,000.00
DigiLog	Arduino Uno	1	PKR 1,900.00
DigiLog	suction Pump1	1	PKR 750.00
DigiLog	IR LED	10	PKR 150.00
DigiLog	RED LED	10	PKR 100.00
DigiLog	DHT 11	2	PKR 400.00
DigiLog	Air quality detector	1	PKR 700.00
DigiLog	LDR light sensor	2	PKR 180.00
DigiLog	Analog to digital converter	3	PKR 330.00
DigiLog	Delivery charges	2	PKR 550.00
Dynamic solution	Arduino Nano	1	PKR 1,850.00
Dynamic solution	LCD	1	PKR 850.00
Dynamic solution	PMS 5003	1	PKR 11,000.00
Dynamic solution	DHT 11	1	PKR 450.00
Dynamic solution	veroboard	1	PKR 250.00
Dynamic solution	header	1	PKR 50.00
Dynamic solution	GPS module	1	PKR 1,450.00
Dynamic solution	Fan	1	PKR 350.00
Dynamic solution	Variable	1	PKR 10.00
Dynamic solution	RGB LED	2	PKR 300.00
Dynamic solution	LDR	2	PKR 200.00
Dynamic solution	IR (transmitter)	2	PKR 200.00
Dynamic solution	IR (reciever)	2	PKR 200.00
Dynamic solution	PVC pipes	1	PKR 1,000.00
Dynamic solution	BOX for components	1	PKR 1,200.00
Dynamic solution	Slits (filter)	2	PKR 600.00
Dynamic solution	Pipe	1	PKR 300.00
Rizwan Sanitary store	PVC pipe	1	PKR 220.00
Rizwan Sanitary store	Pipes C shaped attachement	2	PKR 180.00
Qamar Enterprices stel works	Device casing/Box (Steel sheets + welding + powder coating)	1	PKR 10,000.00
		Total	PKR 42, 742.00